Diversity of Integrative and Conjugative Elements of Streptococcus salivarius and Their Intra- and Interspecies Transfer

Narimane Dahmane, Virginie Libante, Florence Charron-Bourgoin, Eric Guédon, Gérard Guédon, Nathalie N. Leblond-Bourget, Sophie Payot

Diversity of integrative and conjugative elements of *Streptococcus salivarius* and their intra- and interspecies transfer

Running title: Diversity and functionality of ICEs in *S. salivarius*

Narimane Dahmane [1], Virginie Libante [1], Florence Charron-Bourgoin [1], Eric Guédon [2], Gérard Guédon [1], Nathalie Leblond-Bourget [1] and Sophie Payot [1 #]

[1] DynAMic, Université de Lorraine, INRA, 54506, Vandœuvre-lès-Nancy, France;

[2] STLO, Agrocampus Ouest, INRA, 35000, Rennes, France

Corresponding author

Tel: +33 3 72 74 56 81

Fax: +33 3 72 74 53 56

E-mail address: sophie.payot-lacroix@inra.fr

ABSTRACT:

Integrative and Conjugative Elements (ICEs) are widespread chromosomal mobile genetic elements, which can transfer autonomously by conjugation in bacteria. Thirteen ICEs with a conjugation module closely related to that of ICE*St3* of *Streptococcus thermophilus* were characterized in *Streptococcus salivarius* by whole genome sequencing. Sequence comparison highlighted ICE evolution by shuffling of 3 different integration/excision modules (for integration in the 3'end of *fda*, *rpsI* or *rpmG* genes) with the conjugation module of the ICE*St3* subfamily. Sequence analyses also pointed out a recombination occurring at *oriT* (likely mediated by the relaxase) as a mechanism of ICE evolution. Despite a similar organization in 2 operons including three conserved genes, the regulation modules show a high diversity (about 50% of amino acid sequence divergence for the encoded regulators and presence of unrelated additional genes) with a probable impact on the regulation of ICE activity.

Concerning the accessory genes, ICEs of the ICE*St3* subfamily appear particularly rich in restriction-modification systems and orphan methyltransferase genes. Other cargo genes that could confer a selective advantage to the cell hosting the ICE were identified, in particular genes for bacteriocin synthesis and cadmium resistance.

The functionality of 2 ICEs of *S. salivarius* was investigated. Autonomous conjugative transfer to other *S. salivarius* strains, to *S. thermophilus* and to *Enterococcus faecalis* was obtained. The analysis of the ICE-*fda* border sequence in these transconjugants allowed the localization of the DNA cutting site of the ICE integrase.

IMPORTANCE

The ICE*St3* subfamily of ICEs appears to be widespread in streptococci and targets diverse chromosomal integration sites. These ICEs carry diverse cargo genes that can confer a selective

advantage to the host strain. The maintenance of these mobile genetic elements likely relies in part on self-encoded restriction-modification systems.

Here intra and interspecies transfer were demonstrated for 2 ICEs of *S. salivarius*. Closely related ICEs were also detected *in silico* in other *Streptococcus* species (*S. pneumoniae* and *S. parasanguinis*) thus indicating that diffusion of ICE*St3*-related elements probably plays a significant role in HGT occurring in the oral cavity but also in the digestive tract where *S. salivarius* is present.

INTRODUCTION

Acquisition of genes by horizontal gene transfer (HGT) is a major driving force for evolution of bacterial genomes (1, 2). The main mechanism is conjugation, a process that enables transfer of large DNA fragments without requiring any similarity between sequences thus being naturally broad host range (3). Besides conjugative transfer of extrachromosomal elements (plasmids), recent analyses revealed that many integrated mobile elements, called Integrative and Conjugative Elements (ICEs), also encode their own transfer by conjugation (4, 5). Like all other mobile genetic elements (MGEs) (6), ICEs have a modular structure. Three modules, a recombination module, a conjugation module and a regulation module, altogether control and ensure the excision and transfer of the element (7). ICEs are able to excise from the bacterial chromosome generally by site-specific recombination, to transfer using their own conjugative machinery and to integrate in the chromosome of a recipient cell (4, 5). Moreover, various ICEs can promote the transfer of large fragments of the bacterial chromosome by an Hfr-like mechanism (8). They can also mobilize non autonomous integrated transferable elements such as (i) Integrative and Mobilizable Elements (IMEs), genetic elements unrelated to ICEs that can excise/integrate from the chromosome but need to hijack the transfer machinery of a conjugative element or (ii) Cis Mobilizable Elements (CIMEs), elements that derive from ICEs and IMEs by deletion of the conjugation/mobilization and recombination modules but retain recombination sites *att* (4). In this latter case, an ICE that integrates in a recombination site of a CIME can mobilize the non autonomous element by mediating the excision of the whole composite element (process of accretion-mobilization) (9, 10). Multiplication of bacterial genome sequencing projects in the last few years provides a remarkable opportunity to explore the pool of bacterial genetic mobile elements ("mobilome"). These *in silico* analyses revealed the high abundance of ICEs in bacteria (11-13). In addition to the genes involved or controlling their mobility, ICEs also carry

cargo genes, which can provide new properties (virulence, antibiotic resistance for example) to the recipient cell (7).

Streptococcus salivarius is a Firmicute that is a major constituent of the human oral cavity microbiota (14) and is commonly detected in the human gastrointestinal tract of healthy individuals (15, 16). Few strains have also been associated with opportunistic infections in particular in cases of meningitis (17), endocarditis (18) and bacteremia in immunocompromised patients (19, 20). Analyses of *S. salivarius* genomes pointed out the considerable variability of gene content and the differences in adaptive traits (21). Evidence of widespread HGT was obtained in link with the presence of diverse MGEs (21) and the competence for natural transformation of the species (22).

We recently screened a collection of 138 strains of *S. salivarius* for the presence of MGEs (23). This led to the identification of 60 strains (belonging to 39 MLST groups) with a positive PCR signal for the relaxase gene of ICE*St3*, an ICE previously characterized in the closely related species *Streptococcus thermophilus* (24-26). This indicated the presence in these strains of putative ICEs belonging to the ICE*St3* subfamily. However, not all these strains showed a positive PCR signal for the ICE*St3* integrase gene that catalyzes the integration into the *fda* site. This suggested the presence of other recombination modules associated with the ICE*St3* conjugation module in *S. salivarius* ICEs.

In this work, we selected 13 strains with different MLST patterns (including 6 strains with a negative PCR signal for the ICE*St3* integrase gene) and sequenced their genome in order to gain access to their ICE sequences. ICEs with a conjugation module closely related to the one of ICE*St3* were searched in other NCBI available genomes of *S. salivarius* and in other genomes of Firmicutes. ICE sequences were compared and the putative function encoded by their genes was analyzed *in silico*. Two putative ICEs from *S. salivarius* were analyzed experimentally to test their excision and their autonomous intraspecies and interspecies conjugative transfer.

MATERIAL AND METHODS

Bacterial strains, plasmids and culture conditions

The strains and plasmids used in the experimental part of this study are listed in Table 1.

Thirteen *S. salivarius* strains including 4 commensal (F1-4, F1-8, F4-2 and F6-1) and 9 clinical (B35, B57, L22, L50, L60, L64, N5, N20 and T93) were selected on the basis of a previous work (23). These strains were chosen according to 3 criteria. Firstly, the selected strains likely harbor an ICE with a conjugation module related to ICE*St3* (as suggested by a positive PCR signal for the relaxase and coupling protein genes of ICE*St3*). Secondly, to increase the diversity of ICEs included in the analysis, half of the strains were selected according to the absence of a PCR signal for the integrase gene of ICE*St3* thus suggesting the presence of a different recombination module. Lastly, the selected strains are distributed all over the phylogenetic tree built from MLST data (23). They belong to different MLST groups and differ by at least 3 MLST alleles (out of 6 alleles analyzed) and can thus be considered as unrelated, except two of them (strains L22 and L64) which differ by only 1 allele (23). These 13 strains are available upon request.

Modified strains were named according to the modification. For example, *S. salivarius* F1-8 (pMG36e) corresponds to a derivative of *S. salivarius* F1-8 carrying the plasmid pMG36e. pMG36e is a small plasmid (3611 pb) that carries only genes required for its replication and an erythromycin resistance gene. It is a non conjugative plasmid derived from pWV01 that is a broad spectrum plasmid replicating in *E. coli* and in Firmicutes (27) and has been successfully used for labeling recipient strains in conjugation experiments with *S. thermophilus* (24). *S. salivarius*, *E. faecalis* and *S. thermophilus* were grown in M17 broth supplemented with 0.5% lactose (LM17) at 37°C (*S. salivarius*, *E. faecalis*) or 42°C (*S. thermophilus*) without shaking. Selective mitis salivarius agar (MSA; Difco) containing a 1% (wt/vol) tellurite solution, brain heart infusion (BHI; Difco) and

125 reconstituted skim milk broths were also used for mating assays. Solid cultures were made in
126 oxygen-free environment induced by GasPak utilization (BioMérieux).
127 When required, cultures were supplemented with the following antibiotics: chloramphenicol (5 µg
128 ml^{-1} for *S. thermophilus* or 8 µg ml^{-1} for *S. salivarius* and *E. faecalis*); erythromycin (5 µg ml^{-1} for
129 *S. thermophilus* or 10 µg ml^{-1} for *S. salivarius* and *E. faecalis*).
130 **DNA sequencing and sequence analysis**
131 The 13 selected *S. salivarius* strains were subjected to whole genome sequencing. Sequencing was
132 made using Illumina HiSeq2000 sequencer by Beckman Coulter genomics (2×100 pb after paired-
133 end library construction, expected at least 60 × coverage). Observed sequencing depth was higher
134 than 200 × for all the 13 genomes. *De novo* assembly was performed using CLC Genomics
135 Workbench (CLC Bio) using default parameters. Scaffold of the genomes was built by using the
136 Genome Finishing module of CLC Genomics Workbench with *S. salivarius* JIM8777 genome as
137 reference. Some assembly gaps were filled by doing PCR and sequencing. This enabled to obtain
138 genomes fragmented in less than 75 contigs (less than 30 contigs for two thirds of the genomes;
139 median size of the contigs higher than 40 kb for half of them). Contigs were first annotated using the
140 RAST annotation server (http://rast.nmpdr.org/) (28, 29). Then, contig(s) containing genes closely
141 related to conjugation genes of ICE*St3* were identified by BlastN analysis (using *orfO-orfA* genes as
142 query by megaBlast analysis with default parameters and filter disabled) and annotation was
143 completed manually.
144 In NCBI sequence databanks, ICEs closely related to ICE*St3* were searched by using Microbial
145 nucleotide blast (using *orfO-orfA* genes as query by megaBlast analysis with default parameters and
146 filter disabled) on complete (n=816, last accessed 2016/07/29) and draft (n=9573, last accessed
147 2016/07/29) genomes of Firmicutes. Hits with more than 90% of identity with the whole query
148 sequence were further analyzed.

149 Pairwise comparisons of elements were performed with Artemis Comparison Tool provided by the
150 Sanger Centre using comparison files generated by Double Act (available at: http://www.hpa-
151 bioinfotools.org.uk/pise/double_act.html) (30). Manual editing of comparison figures was performed
152 using Inkscape.

153 **Nucleotide sequence accession numbers**

154 The sequences of ICEs have been deposited in the EMBL Nucleotide Sequence Database under
155 accession numbers LT622825-LT622837.

156 **Phylogenetic tree construction**

157 Proteins of twenty-seven ICEs were included in the analysis. These ICEs correspond to (i) the 19
158 ICEs of the ICE*St3* subfamily with closely related conjugation modules and (ii) 8 additional ones
159 previously reported to belong to the same ICE subfamily but showing more distantly related
160 conjugation modules (11, 26). The sequences of signature proteins were aligned using Clustal omega
161 with default parameters (31). The trees were built with MEGA (32) using (i) maximum likelihood
162 (ML) based on JTT (Jones-Taylor-Thornton) model including amino acid empirical frequencies
163 (partial deletion of gaps and missing data at 80% cutoff, Gamma distribution in 5 categories,
164 allowance for invariant sites), and (ii) BioNJ methods with the Poisson model (33). The branch
165 support of the groupings was estimated using bootstrap (100 replicates).

166 **ICE tagging**

167 ICE_*SsaF1-4_fda* and ICE_*SsaF4-2_fda* were tagged by a chloramphenicol resistance cassette
168 originating from pSET5s plasmid. The resistance cassette was inserted in an intergenic region
169 located between convergent coding sequences in the adaptive module to avoid impacting ICE
170 functionality. Two DNA fragments of about 1,000 bp corresponding to the upstream and the
171 downstream regions of the integration locus were amplified by PCR using specific primers that
172 present an extended sequence matching with the 5' and the 3'ends of the chloramphenicol resistance

cassette. A second PCR amplification was carried out using these two PCR fragments and the resistance gene as a template to synthesize a fragment carrying the antibiotic resistance cassette flanked by the upstream and downstream chromosomal regions of the gene. Natural competence of *S. salivarius* cells was induced by addition of the synthetic peptide (H2N – LPYFTGCL – COOH) (22) and the overlap PCR product was then added for transformation. The cross-over events, upstream and downstream from the tagged region, were positively selected by the newly acquired antibiotic resistance of the transformed clones. The integrity of the regions flanking the antibiotic cassette was confirmed by PCR.

PCRs were done using the Phusion high-fidelity DNA polymerase (Thermo Scientific). PCRs were performed with 50 ng of genomic DNA, 200 µM of each deoxynucleotide triphosphate (dNTP), 0.5 µM of each primer (for primer sequences, see Table 2) and 0.02 U μl^{-1} of Phusion DNA polymerase in appropriate buffer per 50 µl reaction volume. Cycling conditions for the overlap PCR were: 3 min at 98°C, 30 s at annealing temperature (with 1°C of incrementation at each cycle), 30 s/kb at 72°C, followed by 30 additional cycles with an annealing temperature of 55°C and a final extension of 10 min at 72°C.

Excision tests with or without mitomycin C (MMC)

PCR amplifications of *attB*, *attI*, *attR* and *attL* fragments were carried out in a 25 µl volume containing 1 µl of overnight culture, 200 µM of each dNTP (Thermo Scientific, France), 0.5 µM of each primer (for primer sequences, see Table 2), and 0.025 U μl^{-1} of DreamTaq DNA polymerase in an appropriate buffer (Thermo Scientific, France). PCR amplifications were performed using the following cycling parameters: 10 min at 95°C, followed by 30 cycles of 30 s at 95°C, 30 s at 50°C, and 1 min/kb at 72°C, with a final 5-min extension at 72°C. Amplified products were analyzed by electrophoresis on a 1.5% agarose gel.

To test the impact of mitomycin C on the ICE excision, PCR amplifications of the attachment sites were done after a 2.5 h-treatment of the cells with MMC. To select the MMC concentration that gives the highest induction of excision, a range of MMC concentrations (0.025 to 0.4 mg ml^{-1}) was first tested using 1 ng of genomic DNA as template. Semi-quantitative PCR (performed with 30 cycles) were then done at the selected concentration of MMC (0.05 mg ml^{-1}) using different genomic DNA quantities (0.1 µg to 1 pg). Amplifications of the *fda* gene were done in parallel as controls.

Mating experiments

Donor and recipient strains were grown overnight with an appropriate antibiotic. 15 ml of broth medium were inoculated with 150 µl of donor or recipient stationary phase cultures. Cultures were grown until mid-exponential phase (optical density at 600 nm of 0.4), then were mixed and centrifuged for 15 min in a prewarmed centrifuge at 4,500 × g to pellet cells. The pellet was resuspended in 1 ml of LM17 broth and 150 µl were spread on 0.45 µm pore-size cellulose nitrate filters (Sartorius stedim biotech) deposited on LM17 soft agar (0.8 %) plates. Plates were then incubated at 37°C (for *S. salivarius*/*S. salivarius* and *S. salivarius*/*E. faecalis* mating pairs) or at 39°C (for *S. salivarius*/*S. thermophilus* mating pairs). After an overnight incubation, the filters were removed from the agar plates and placed into 10 ml of LM17 liquid media. Bacteria were recovered by vortexing for 30 s. The suspension was then directly spread on agar plates supplemented with the appropriate antibiotics or concentrated 10 times by centrifugation at 4,500 × g for 15 min to enable counting the CFUs of the donor, the recipient, and the transconjugants cells after a 24h-incubation. Transconjugants clones obtained after *S. salivarius* intraspecies mating were typed by DNA sequencing of PCR products corresponding to the *ddlA* gene (for primer sequences, see Table 2).

Treatment of donor cells with mitomycin C (MMC) was done as follows: cells carrying ICE*_SsaF1-4_fda* were grown in LM17 liquid medium at 37°C to an optical density at 600 nm of 0.4. The culture was then diluted 10-fold in 15 ml of prewarmed LM17 containing MMC at the

concentration that showed the maximum ICE excision level (0.05 mg ml^{-1}). A 10-fold dilution without MMC was used as a control. After 1 hour of culture, the cells were harvested by centrifugation in a prewarmed centrifuge and washed once with 15 ml of prewarmed LM17. The donor cells treated with MMC were mixed with recipient cells grown at optical density at 600 nm of 0.4 and centrifuged for 15 min in a prewarmed centrifuge at 4,500 × g to pellet cells. The pellet was resuspended in 1 ml of LM17 broth, and 150 µl were spread on nitrocellulose filter on LM17 soft agar plates before incubation for 4h or overnight at appropriate temperatures. The filters were then treated as previously described.

Mating frequencies were calculated by dividing the number of transconjugants by the number of donor cells, except in the case of donor cells treated with MMC, where mating frequencies were calculated relative to recipients. At least three independent biological replicates were done.

Plasmid curing

Transconjugants carrying plasmid pMG36e were cultured overnight without erythromycin, and were then spread on LM17 plates at different dilutions. One hundred isolated clones were then streaked on LM17 plates with or without erythromycin. Erythromycin sensitive clones were then confirmed by PCR for the absence of plasmid (see Table 2 for primer sequences).

Random Amplification of Polymorphic DNA (RAPD)

RAPD (34) was carried out with DreamTaq enzyme (for primer sequences see Table 2). Cycling conditions were: 40 cycles consisting of 94°C for 1 min, 31°C for 1 min, and 72°C for 2 min; the final extension was continued for 7 min at 72°C. 1 µl of liquid culture was used as DNA template. The PCR products were separated by electrophoresis on a 1.5% agarose gel.

RESULTS AND DISCUSSION

Diversity of Integrative and Conjugative Elements of the ICE*St3* subfamily identified in *S. salivarius* and in other streptococci

Conjugation modules

To explore the diversity of the ICEs of the ICE*St3* subfamily found in *S. salivarius*, 13 strains (F1-4, F1-8, F4-2, F6-1, B35, B57, L22, L50, L60, L64, N5, N20 and T93) with different MLST patterns were selected from a previous work (23) (Table 1). These strains likely encode an ICE of the ICE*St3* subfamily as suggested by a positive PCR signal for the ICE*St3* relaxase gene (23). Their genome was sequenced and assembled in order to gain access to their ICE sequences. Except for 2 ICEs (ICE_*SsaF6-1_rpsI* and ICE_*SsaB57_fda*) split into 2 contigs, the sequences of the ICEs appear on a single contig (Fig. 1). As shown in Fig. 1, ICEs found in these 13 *S. salivarius* strains all display a conjugation module that is closely related to that of ICE*St3* from *S. thermophilus* (>90% of nucleic sequence identity). ICEs with a closely related full conjugation module were also detected in 2 genomes of *S. salivarius* available in NCBI (those of strains JF and 1270) (Fig. 1). The element of *S. salivarius* NCTC 8618 (GenBank accession number: CP009913.1) also has a closely related full conjugation module but is not shown in the figure since it harbors a truncated integrase gene, and is therefore defective. Elements with a closely related conjugation module (partial in most of the genomes due to gaps in the assembly) were also detected in the genomes of strains GED7778A (GenBank accession number LRQS00000000), 140 (GenBank accession number: JVSQ01000000), 20-02 S1 (GenBank accession number: LXMB00000000), 20-12 S2 (GenBank accession number: LXMC00000000) and UC3162 (GenBank accession number: JYOY01000000). These elements are not shown in Fig. 1 because their sequence is incomplete. ICEs with a closely related conjugation module (92-94% of nucleic sequence identity with that of ICE*St3*) were also identified in the genome

of *Streptococcus pneumoniae* 2842STDY5753514 (mitis group) and *Streptococcus parasanguinis* DD19 (sanguinis group) (Fig. 1). Phylogenetic analysis of the relaxase OrfJ (Fig. 2) and the coupling protein OrfK (Fig. 3) of these ICEs indicates that they group with OrfJ and OrfK from *S. salivarius* ICEs. Similar results were obtained for the other proteins of the conjugation module (data not shown). Taken as a whole, these phylogenetic analyses and sequence comparisons clearly showed that transfers of ICEs closely related to ICE*St3* have occurred between distinct species from different streptococcal groups.

The comparison of the clustering groups obtained for the relaxase (OrfJ) and the coupling protein (OrfK) indicated that OrfJ of ICE*_Sma33MO_fda* is closely related to the relaxases of ICE*St3* and *S. salivarius* ICEs whereas OrfK is clearly different from the coupling proteins of these ICEs, but is closer to that of ICE*_SparauNCFD2020_rpsI* (see phylogenetic trees in Fig. 2 and 3). Nucleic sequence alignments indicated that the left extremity of the conjugation module (including *orfN* to *orfK* genes) of ICE*_Sma33MO_fda* is closely related to the corresponding sequence of ICE*_SparauNCFD2020_rpsI* (86% of nucleic sequence identity compared to 64% of nucleic sequence identity with the corresponding genes of ICE*St3*) whereas the right extremity of the conjugation module of ICE*_Sma33MO_fda* (corresponding to *orfJ* to *orfA* genes) is closely related to those of ICE*St3* (96% of nucleic sequence identity compared to 64% of nucleic sequence identity with the corresponding genes of ICE*_SparauNCFD2020_rpsI*) and *S. salivarius* ICEs. The putative *nic* site of the transfer origin of ICEs of the ICE*St3* subfamily, predicted by comparison with the *oriT* characterized for ICE*Bs1* of *Bacillus subtilis* (35), is located between *orfK* and *orfJ* genes (supplementary Fig. S1). Sequence alignment of this region indicated that the drop in nucleic sequence identity between ICE*_Sma33MO_fda* and ICE*_SparauNCFD2020_rpsI* occurs at the *nic* site (supplementary Fig. S1). This suggests that a recombination event occurred at *oriT* in ICE*_Sma33MO_fda*. This *oriT* recombination was likely mediated by the relaxase of the ICE that is

able to recognize and nick this sequence. Such *oriT* site-specific recombination has already been demonstrated for several canonical relaxases of plasmids (belonging to MobF, MobP, MobC and MobM families) (4, 36, 37) and has been suggested to occur in ICEs of the SXT/R391 family and for ICE*clc* (both encoding canonical relaxases of the MobH family) (38, 39). This mechanism that enables to create hybrid ICEs could thus also be mediated by relaxases of the non-canonical MobT family, which are related to rolling circle replication initiators and are found in ICEs of the Tn*916*/ICE*St3*/*ICEBs1* family, a family of ICEs widespread in streptococci (11) and other Firmicutes (5).

Integration modules

ICE*St3* conjugation modules found in *S. salivarius* ICEs are associated with 3 different recombination modules (see supplemental Figure S2) enabling integration of the corresponding ICEs in the 3' end of three different genes: *fda* (encoding the fructose-1-6-diphosphate aldolase, as for ICE*St3*), *rpsI* (encoding the S9 ribosomal protein) and *rpmG* (encoding the L33 ribosomal protein). This confirms our previous results showing a positive PCR signal for ICE*St3* relaxase gene but not for ICE*St3* integrase gene for 22 strains (23). Closely related integrases were found in ICEs of *S. salivarius* strains that are distant in the phylogenetic tree built on the basis of MLST data (for example in strains F1-4, L22 and N5 or in strains B35/L50) (23) but also in ICEs found in other species (for example in *S. pneumoniae* 2842STDY5753514 or in *S. parasanguinis* DD19 and *S. macedonicus* 33MO) (supplemental Figure S2). This is in agreement with the previously reported exchanges of recombination modules in ICE*St3* subfamily (11, 26).

Regulation modules

Comparison of the regulation modules of all ICEs of the ICE*St3* subfamily showed their high diversity (Fig. 1). The only common characteristic is the presence, in most of the ICEs, of homologs of *arp1*, *orfQ* and *arp2* genes. This strongly suggests that these genes participate to the same regulation cascade and likely interact/interfere with each other. Exceptions are ICE*_SsaL60_rpsI* devoid of *arp1* gene, ICE*_SsaB35_rpsI* lacking the *orfQ* gene and ICE*_SpaDD19_fda* carrying truncated *arp1* and *orfQ* genes. ICE*_SsaN20_rpsI* also displays a peculiar regulation organization, with full copies of *arp1* and *orfQ* genes separated by truncated copies of *orfQ* and *arp1* genes. This is due to an insertion of genes (including one encoding a transposase) in this region of the ICE (Fig. 1). The *arp1*, *orfQ* and *arp2* genes encode respectively a cI-related repressor, a ImmA-related putative protease (40) and a putative transcriptional regulator (41) that are related to those of ICE*St3* from *S. thermophilus* (26, 42). Arp1 and Arp2 homologs all share an N-terminal helix-turn helix PF01381 domain that is found in several regulatory proteins including Cro and cI regulators of the λ phage. Arp1 proteins also display a C-terminal PF00717 peptidase S24-like domain involved in the autocleavage of the cI repressor induced by DNA damage. OrfQ homologs are characterized by a COG2856 Zn-dependent peptidase ImmA domain, also found in the ImmA protease of ICE*Bs1* of *B. subtilis* that cleaves the ImmR repressor in response to DNA damage (40). A high diversity is observed in the nucleotide (Fig. 1) and amino acid primary sequences of the encoded regulators. Up to 45%, 58% and 53% of divergence was observed between the sequences of Arp1, OrfQ and Arp2 proteins encoded by ICEs of *S. salivarius*. If considering only the ICEs that harbor the *arp1*, *orfQ* and *arp2* genes, the sequence divergence goes from 5 to 37% for Arp1, 7 to 58% for OrfQ and 7 to 37% for Arp2.

In support of a modular evolution of ICEs that was already noticeable from the exchanges in the recombination modules mentioned previously, some ICEs harbor regulators which are distantly related to those found in the other ICEs of *S. salivarius* despite having a closely related conjugation

module (deduced from the phylogenetic trees of relaxases and coupling proteins). This is the case of ICE*_SsaF4-2_fda* that has a conjugation module closely related to the one of ICE*St3* (94% of nucleic sequence identity over the whole conjugation module) but encode more distant regulators (with 63, 46 and 73% of amino acid identity with those encoded by ICE*St3* for Arp1, OrfQ and Arp2 respectively).

Furthermore, all the regulation modules include additional genes (1 to 3 depending on the ICE) between the *arp2* and *orfQ* genes. These genes that encode proteins of unknown function contribute to the diversity of the regulation modules.

Accretions

Accretion of ICEs with other genetic elements was observed: ICEs of strains F1-8 and L60 are in accretion with a putative IME, whereas those of strains F6-1 and L50 are adjacent to 1 or 2 CIMEs (data not shown).

Evidences of accretion or recombination events were also found in the sequence of several ICEs of *S. salivarius*. A truncated supplementary copy of the *orfA* gene was found between *orfA* and the excisionase genes in *S. salivarius* L22 and B57 ICEs and in the closely related ICE found in *S. parasanguinis* DD19. The presence of supplementary truncated *arp1* and *orfQ* genes and of a transposase gene was also detected in the regulation module of *S. salivarius* N20 ICE. These structures could result from (i) the integration of an ICE within an *att* site flanking a resident element (accretion) or (ii) by recombination between ICEs, followed by internal deletion(s) in both cases. These mechanisms contribute to the plasticity and evolution of ICEs and potentiate gene transfer mediated by these MGE.

Cargo genes found on ICEs of the ICE*St3* subfamily in *S. salivarius* and other streptococci

A diversity of cargo genes was found in the left part of the ICEs of the ICE*St3* subfamily explaining the variation of their size ranges: from 25.8 kb for the smallest one (ICE*_SsaL64_fda*) to 37.3 kb for the largest one (ICE*_SsaN20_rpsI*) (Fig. 1). The 2 closely related strains included in the analysis (L22 and L64) harbor ICEs with unrelated cargo genes (Fig. 1). In addition, ICEs found in unrelated strains of *S. salivarius* (for example in strains JF and L22 or F4-2 and F1-8) or in different species (in *S. salivarius* T93 and *S. parasanguinis* DD19) harbor the same cargo genes (Fig. 1). This distribution is due to the horizontal transfer of these genes (exchange of module between ICEs or transfer of the whole ICE).

Two thirds (13/19 if including ICE*St3* (43)) of the ICEs analyzed in this work carry a restriction-modification (RM) system (n=6) or an orphan methyltransferase (n=7) (Fig. 1). This is in accordance with a previous study indicating that the abundance of RM systems correlates with the presence of MGEs in small genomes (44). RM systems were first described as bacterial innate immune systems allowing protection against foreign unmethylated DNA (45). Unmethylated incoming DNA will be degraded by restriction enzymes produced by the cell while the genome of the host remains protected due to methylation by the cognate methyltransferase. RM systems carried by ICEs of *S. salivarius* could protect their host from invasion by other genetic elements such as phages, thus playing a role in “cellular defense” as described for other bacteria (46-48). RM systems also turn out to be selfish mobile elements themselves (49). RM systems that carry the restriction enzyme activity and modification enzyme activity on separate proteins (as observed for the ICEs of the ICE*St3* subfamily) can have an impact on the maintenance of the MGE carrying them (mechanism of genetic addiction). The MGE encodes the poison endonuclease activity and its “antidote”, the methyltransferase (45). Post-segregational killing would occur if the whole RM system is lost. Dilution of the modification enzyme by cell division will lead to the exposure of unmethylated recognition sites on newly replicated chromosomes that will be targeted by the restriction enzyme.

385 Only a few remaining molecules of restriction enzymes are sufficient to kill the cell. Concerning
386 orphan methyltransferases (encoded by 7 of the ICEs of the ICE*St3* subfamily analyzed in this work),
387 if these enzymes target the same DNA sequence as a resident RM system, they could protect the host
388 from post-segregational killing thus participating in the displacement of the resident MGE (50).
389 Two ICEs found in *S. salivarius* L60 and N20 carry a cadmium resistance cluster (*cadD*/*cadX*) (Fig.
390 1). Cadmium is a widespread heavy-metal air pollutant which is commonly released into the
391 environment from industrial processes (in particular glass manufacturing) and urban activities, as
392 well as from the widespread application of fertilizers, manures and sewage sludge (51). The
393 *cadD*/*cadX* genes also appear in a CIME in accretion with the ICE from strains F6-1 and L50 (data
394 not shown). In these latter ones, full recombination sites are still present and thus the CIME and the
395 ICE are considered separately. In these strains, the whole CIME-ICE composite element could excise
396 and transfer by a process of accretion-mobilization already demonstrated with other ICEs of this
397 family (9, 10). Sequence comparison revealed 98% of nucleic identity over 2683 bp between the
398 CIME located upstream of the ICE in strain L50 and the region that includes *cadD*/*cadX* genes in
399 ICE*_SsaL60_rpsI*. This suggests that in strain L60 the cadmium resistance cluster was acquired by
400 the ICE after deletion of the recombination site delimiting the ICE and the adjacent CIME. This
401 mechanism contributes to the plasticity and evolution of ICEs as previously suggested (4).
402 ICE*_SsaF6-1_rpsI* carries a cluster of genes (10.8 kb) that could be involved in membrane lipid
403 synthesis. It includes in particular a *fabF*-like gene encoding a beta-ketoacyl-[acyl-carrier-protein]
404 synthase II (KASI/IIcd00834 domain with E=1.4e-144) and a KBL_like gene encoding a serine
405 palmitoyltransferase involved in sphingolipid synthesis (cd06454 domain with E=3.7e-151).
406 Two ICEs (found in the unrelated strains *S. salivarius* JF and L22) harbor a closely related cluster of
407 genes (*slv* cluster, 15.7 to 15.9 kb) involved in the biosynthesis of a bacteriocin (salivaricin D). These
408 clusters differ from the one previously described in the commensal strain 5M6c of *S. salivarius*

isolated from a healthy infant (52) by the number of copies of the *slvD* structural gene (2 and 3 identical copies respectively compared to 1 in strain 5M6c). Salivaricin D is a nisin-like lantibiotic with a broad-spectrum that includes a large array of Gram positive bacteria in particular the important pathogens *S. pneumoniae* and *S. pyogenes* (52). Thus, it could be used as a potential weapon, for commensal species of the oral cavity such as *S. salivarius*, to compete with oronasopharynx-colonizing streptococci including pathogens (52-54). Bacteriocins could also play a role of addiction system by killing neighboring cells that do not encode resistance to the bacteriocin and thus contribute to the maintenance of the MGE in the population (55).

The ICE found in *S. macedonicus* 33MO carries genes that encode cell-envelope proteins: one with a PF03780 domain with cell envelope-related function (E=7.93e-23), and 3 membrane proteins. Lastly, ICEs of *S. salivarius* T93 and *S. parasanguinis* DD19 harbor the same cargo genes, in particular (i) a two-component system with a signal transduction histidine kinase (nitrate/nitrite-specific COG3850 NarQ domain, E=5.3e-13) and a NarL DNA-binding response regulator (COG2197 domain, E=6.1e-48) and (ii) a cluster of genes encoding a putative LolCDE complex which catalyzes the release of lipoproteins from the cytoplasmic membrane (LolC PF13521 AAA_28 domain, E=1.2e-09; LolD cd03255 ABC_MJ0796_LolCDE_FtsE domain, E=1.2e-108 and LolE COG4591 domain, E=4.4e-14) (Fig. 1).

Excision tests of 2 putative ICEs: ICE*_SsaF1-4_fda* and ICE*_SsaF4-2_fda*

Experiments were carried out to test the functionality of 2 putative ICEs of *S. salivarius*. The first one, ICE*_SsaF1-4_fda*, has a conjugation module showing the highest percentage of identity with that of ICE*St3* of *S. thermophilus*, an ICE whose transfer was previously demonstrated (24) (Fig. 1). Arp1, OrfQ and Arp2 regulators encoded by this ICE are also closely related to those of ICE*St3* (85, 71 and 84% of amino acid identity respectively). As mentioned before, the second one, ICE*_SsaF4-*

433 *2_fda*, has a conjugation module closely related to ICE*_SsaF1-4_fda* and ICE*St3* but harbors a
434 distantly related regulation module.
435 Excision of these 2 ICEs was tested by PCR. Amplifications were obtained for *attI* and *attB*
436 corresponding to the circular excised form and the empty chromosomal site respectively, indicating
437 the functionality of their recombination module. Recombination sites (*attL* and *attR*) flanking the
438 ICEs were also amplified (data are shown only for ICE*_SsaF1-4_fda*, Fig. 4).
439
440 **Test of intraspecies conjugative transfer of 2 putative ICEs of *S. salivarius***
441 Both ICE*_SsaF1-4_fda* and ICE*_SsaF4-2_fda* were first tagged by a chloramphenicol resistance
442 cassette (Table 1). Donor strains were then used in filter mating experiments with two *S. salivarius*
443 recipient strains: JIM8777 and F1-8, displaying different genotypes (Table 1 and 3). Both strains
444 carry an empty *fda* integration site and strain F1-8 carries an ICE belonging to the ICE*St3* subfamily
445 (Fig. 1) in accretion with an IME integrated in the 3' end of *rpmG*. Some putative transconjugants
446 were recovered when JIM8777 or F1-8 *S. salivarius* strains were used as recipients (Table 3). After
447 sub-culturing, transconjugants were confirmed by detection of the integrase gene (data are shown
448 only for ICE*_SsaF1-4_fda*, Fig. 5a, 5b). For JIM8777 derivative clones, this screen was combined
449 with detection of the pMG36e plasmid and RAPD (Fig. 5a). F1-8 transconjugants were confirmed by
450 sequencing of an MLST locus (*ddlA* gene). The site specific insertion in the *fda* gene and the
451 excision of the newly acquired ICEs were also confirmed by the PCR detection of *attL*, *attR*, *attI* and
452 *attB* sites for both F1-8 (data are shown only for ICE*_SsaF1-4_fda*, Fig. 5c), and JIM8777 (data not
453 shown). This suggests that the elements are still active in these transconjugants (at least for excision).
454 Mating experiments were repeated with at least 3 different cultures of donor and recipient cells
455 (biological repetitions) but very few transconjugants (2 clones for the whole experiment) were
456 obtained thus preventing any calculation of transfer frequency. Attempts to increase ICE*_SsaF1-*

457 *4_fda* transfer frequency were made: (i) test of different media (milk, BHI, mitis, M17 broth with 1%
458 final glucose instead of 0.5% final lactose), (ii) test of different donor/recipient ratio ranging from
459 1:1, 2:1, 10:1, 50:100 to 100:1, (iii) mix of donor and recipient at the end of exponential growth
460 phase or stationary phase instead of mid-exponential phase. None of the tested conditions enabled to
461 increase transfer frequency which remained inferior to 10^{-8} transconjugants per donor cells.
462
463 **Test of interspecies conjugative transfer of ICEs of *S. salivarius***
464 To evaluate ICE interspecies transfer, mating assays were carried out with two other *Firmicutes* as
465 recipients: the closely related *S. thermophilus* and *Enterococcus faecalis*. Recipient strains were
466 *S. thermophilus* LMG18311 and *E. faecalis* JH2-2 both carrying pMG36e and described as recipients
467 strains of ICE*St3* from *S. thermophilus* (transfer frequency of $3.4 \times 10^{-6} \pm 0.5 \times 10^{-6}$ and $3.9 \times 10^{-7} \pm$
468 0.9×10^{-7} respectively (24)). Some putative transconjugants (2 clones for the whole experiment)
469 were recovered when using strains F1-4 or F4-2 as donors in mating experiments (Table 3) and
470 confirmed by PCR detection of the ICE integrase gene (data are shown only for ICE*_SsaF1-4_fda*,
471 Fig. 6). LMG18311 genetic background was confirmed by PCR amplification of the internal
472 transcribed spacer (ITS) followed by *Hae*III DNA digestion, which allows discriminating
473 *S. salivarius* strains and *S. thermophilus* LMG18311 (data are shown only for ICE*_SsaF1-4_fda*, Fig.
474 6a). JH2-2 genetic background was confirmed by the PCR amplification of the ITS and by the
475 amplification of *fda* gene with primers specific to *E. faecalis* (data are shown only for
476 ICE*_SsaF1-4_fda*, Fig. 6b).
477 ICE*_SsaF1-4_fda* carries 27 bp showing identity with the 3' end region of the *fda* gene of
478 *S. salivarius* (Fig. 7). This sequence (present in *attI*) enables specific recombination with the
479 chromosomal integration site of the recipient cell (*attB* site) and generates a 27 bp-imperfect direct
480 repeat (DR) in intraspecies transconjugants (Fig. 7). Sequencing of the *attR* site obtained after

integration of ICE*_SsaF1-4_fda* in *E. faecalis* JH2-2 recipient cells provided relevant information on the DNA localization of one cutting site of *fda* integrase. This *attR* site is a hybrid between the sequence found in the *attI* of ICE*_SsaF1-4_fda* and the *attB* of *E. faecalis* JH2-2 recipient cells. Since the *attB* sequence in the recipient strains is different from the *attI* of ICE*_SsaF1-4_fda* (Fig. 7), the presence of a T nucleotide at position 20 of the DR in the *attR* of the transconjugants, as in ICE*_SsaF1-4_fda*, indicates that integrase cuts downstream of this nucleotide to allow strand exchange during recombination. A previous work aiming at studying CIME-ICE accretion also identified the same cutting position as well as the position of a second staggered cutting site located 6 bp downstream (Fig. 7) (56).

Intra- and interspecies conjugative transfer of two different ICEs found in *S. salivarius* was obtained in laboratory conditions. These ICEs could thus play a significant role in HGT occurring both in the oral cavity (as exemplified by the presence of a closely related ICE in *S. parasanguinis*) and in the digestive tract.

Impact of mitomycin C on excision and transfer of ICE*_SsaF1-4_fda*

A previous work demonstrated that excision and transfer of ICE*St3* of *S. thermophilus* can be increased by treating donor cells with mitomycin C (42). Hence we examined the impact of such treatment on excision and transfer of an ICE from *S. salivarius* (ICE*_SsaF1-4_fda*). Induction of ICE excision by mitomycin C was tested by PCR amplification of *attI* and *attB* fragments using different amounts of genomic DNA (0.1 µg to 1 pg) after MMC treatment or not of the cells (Fig. 8). The minimal quantity of DNA producing a positive result for *attI* and *attB* was 0.1 ng for non-treated cells whereas 10 pg of DNA were sufficient to detect a signal after MMC treatment of the cells (Fig. 8). Furthermore, when cells were treated with MMC, a higher intensity of the PCR signal was observed for *attI* and *attB* using 0.1, 1 and 10 ng of DNA compared to cells without MMC treatment

(Fig. 8). Such difference was not observed for the *fda* control (Fig. 8). Thus, as for ICE*St3* (42), MMC treatment leads to an increase of ICE*_SsaF1-4_fda* excision.

To evaluate the effect of MMC on ICE transfer, strain F1-4 was treated with MMC (at the concentration inducing the maximum level of ICE excision) and used in filter mating experiments with *S. salivarius* strain F1-8 as recipient. No difference of ICE transfer was detectable between cells treated or not with MMC. This is in contrast to what was observed for ICE*St3* (42). Thus, it appears that for ICE*_SsaF1-4_fda* excision is not a limiting step for transfer.

Retransfer of ICE*_SsaF1-4_fda* from transconjugants

To test whether ICE*_SsaF1-4_fda* transfers autonomously, retransfer was tested by using transconjugants (obtained as described above) as donor cells. Plasmid pMG36e was removed by curing transconjugants prior to the retransfer assays. F1-8 (ICE*_SsaF1-4_fda*) was used as donor cells in filter mating experiments with either F1-8 (pMG36e) or LMG18311 (pMG36e) as recipient cells. LMG18311 (ICE*_SsaF1-4_fda*) and JH2-2 (ICE*_SsaF1-4_fda*) were used as donor cells with LMG18311 (pMG36e) and JH2-2 (pMG36e) respectively (Table 3). For each mating assay, transconjugants were recovered and confirmed by PCR detection of both the ICE integrase gene and the plasmid pMG36e present in the recipients (data not shown). A small number of transconjugant colonies (as for intraspecies transfer of ICE*_SsaF1-4_fda* i.e. 2 clones for the whole experiment) was observed when using *S. salivarius* as donor, and strains with the same genetic background as recipients (F1-8/F1-8 mating pairs) or *S. thermophilus* LMG18311 as recipient cells. By contrast, more transconjugant colonies (at least 20 clones for the whole experiment) were obtained using *S. thermophilus* LMG18311 (ICE*_SsaF1-4_fda*) and *E. faecalis* JH2-2 (ICE*_SsaF1-4_fda*) as donors and LMG18311 (pMG36e) and JH2-2 (pMG36e) as recipient cells. These results confirm that ICE*_SsaF1-4_fda* is able to transfer autonomously but also suggest that (i) host factors could impact

ICE replication or/and assembly of the conjugation machinery in *S. salivarius* as already suggested for some strains of *S. thermophilus* (26), (ii) molecules displayed at the cell surface of *S. salivarius* could impact the donor/recipient cell contacts and thus the assembly of the conjugative machinery. These hypotheses are consistent with the fact that no transconjugant was recovered when *S. thermophilus* CNRZ368 donor cells carrying ICE*St3* were mated with *S. salivarius* JIM8777 or F1-8 recipient cells (data not shown in this study) whereas transconjugants were obtained using *S. thermophilus* LMG18311 as recipient cells as already reported (24).

It should be kept in mind that *S. salivarius* encounters different physiological conditions in the oral cavity and along the digestive tract. The impact on ICE regulation of these complex interactions between bacteria and of changing environment in these ecological niches should be explored in close future.

ACKNOWLEDGMENTS

We thank Stéphane Bertin and Emilie Robert for their technical help.

FUNDING INFORMATION

N.D. is recipient of a scholarship funded by INRA and Région Grand Est (formerly Région Lorraine).

This work received financial support from the Région Lorraine and Université de Lorraine (2011-2013) and ANR (MATICE project <ANR-15-CE21-0007>).

REFERENCES:

1. **Abby SS, Tannier E, Gouy M, Daubin V.** 2012. Lateral gene transfer as a support for the tree of life. Proc Natl Acad Sci U S A **109:**4962-7.
2. **Ochman H, Lawrence JG, Groisman EA.** 2000. Lateral gene transfer and the nature of bacterial innovation. Nature **405:**299-304.
3. **Llosa M, Gomis-Ruth FX, Coll M, de la Cruz Fd F.** 2002. Bacterial conjugation: a two-step mechanism for DNA transport. Mol Microbiol **45:**1-8.
4. **Bellanger X, Payot S, Leblond-Bourget N, Guédon G.** 2014. Conjugative and mobilizable genomic islands in bacteria: evolution and diversity. FEMS Microbiol Rev **38:**720-60.
5. **Roberts AP, Mullany P.** 2013. *In* Roberts AP and Mullany P (ed), Bacterial Integrative Mobile Genetic Elements, Landes Bioscience, Austin, TX.
6. **Toussaint A, Merlin C.** 2002. Mobile elements as a combination of functional modules. Plasmid **47:**26-35.
7. **Burrus V, Pavlovic G, Decaris B, Guédon G.** 2002. Conjugative transposons: the tip of the iceberg. Mol Microbiol **46:**601-10.
8. **Brochet M, Rusniok C, Couvé E, Dramsi S, Poyart C, Trieu-Cuot P, Kunst F, Glaser P.** 2008. Shaping a bacterial genome by large chromosomal replacements, the evolutionary history of *Streptococcus agalactiae*. Proc Natl Acad Sci U S A **105:**15961-6.
9. **Bellanger X, Morel C, Gonot F, Puymege A, Decaris B, Guédon G.** 2011. Site-specific accretion of an Integrative Conjugative Element and a related genomic island leads to cis-mobilization and gene capture. Mol Microbiol **81:**912-925.

10. **Puymège A, Bertin S, Chuzeville S, Guédon G, Payot S.** 2013. Conjugative transfer and cis-mobilization of a genomic island by an Integrative and Conjugative Element of *Streptococcus agalactiae*. J Bacteriol **195:**1142-51.

11. **Ambroset C, Coluzzi C, Guédon G, Devignes MD, Loux V, Lacroix T, Payot S, Leblond-Bourget N.** 2016. New insights into the classification and integration specificity of *Streptococcus* Integrative Conjugative Elements through extensive genome exploration. Front Microbiol **6:**1483.

12. **Guglielmini J, Quintais L, Garcillan-Barcia MP, de la Cruz F, Rocha EP.** 2011. The repertoire of ICE in prokaryotes underscores the unity, diversity, and ubiquity of conjugation. PLoS Genet **7:**e1002222.

13. **Puymège A, Bertin S, Guédon G, Payot S.** 2015. Analysis of *Streptococcus agalactiae* pan-genome for prevalence, diversity and functionality of integrative and conjugative or mobilizable elements integrated in the tRNA(Lys CTT) gene. Mol Genet Genomics **290:**1727-40.

14. **Aas JA, Paster BJ, Stokes LN, Olsen I, Dewhirst FE.** 2005. Defining the normal bacterial flora of the oral cavity. J Clin Microbiol **43:**5721-32.

15. **Qin J, Li R, Raes J, Arumugam M, Burgdorf KS, Manichanh C, Nielsen T, Pons N, Levenez F, Yamada T, Mende DR, Li J, Xu J, Li S, Li D, Cao J, Wang B, Liang H, Zheng H, Xie Y, Tap J, Lepage P, Bertalan M, Batto JM, Hansen T, Le Paslier D, Linneberg A, Nielsen HB, Pelletier E, Renault P, Sicheritz-Ponten T, Turner K, Zhu H, Yu C, Jian M, Zhou Y, Li Y, Zhang X, Qin N, Yang H, Wang J, Brunak S, Dore J, Guarner F, Kristiansen K, Pedersen O, Parkhill J, Weissenbach J, Bork P, Ehrlich SD.** 2010. A human gut microbial gene catalogue established by metagenomic sequencing. Nature **464:**59-65.

16. **Van den Bogert B, Boekhorst J, Herrmann R, Smid EJ, Zoetendal EG, Kleerebezem M.** 2013. Comparative genomics analysis of *Streptococcus* isolates from the human small intestine reveals their adaptation to a highly dynamic ecosystem. PLoS One **8:**e83418.

17. **Wilson M, Martin R, Walk ST, Young C, Grossman S, McKean EL, Aronoff DM.** 2012. Clinical and laboratory features of *Streptococcus salivarius* meningitis: a case report and literature review. Clin Med Res **10:**15-25.

18. **Kitten T, Munro CL, Zollar NQ, Lee SP, Patel RD.** 2012. Oral streptococcal bacteremia in hospitalized patients: taxonomic identification and clinical characterization. J Clin Microbiol **50:**1039-42.

19. **Corredoira JC, Alonso MP, Garcia JF, Casariego E, Coira A, Rodriguez A, Pita J, Louzao C, Pombo B, Lopez MJ, Varela J.** 2005. Clinical characteristics and significance of *Streptococcus salivarius* bacteremia and *Streptococcus bovis* bacteremia: a prospective 16-year study. Eur J Clin Microbiol Infect Dis **24:**250-5.

20. **Han XY, Kamana M, Rolston KV.** 2006. Viridans streptococci isolated by culture from blood of cancer patients: clinical and microbiologic analysis of 50 cases. J Clin Microbiol **44:**160-5.

21. **Delorme C, Abraham AL, Renault P, Guedon E.** 2014. Genomics of *Streptococcus salivarius*, a major human commensal. Infect Genet Evol**:**pii: S1567-1348(14)00372-4.

22. **Fontaine L, Boutry C, de Frahan MH, Delplace B, Fremaux C, Horvath P, Boyaval P, Hols P.** 2010. A novel pheromone quorum-sensing system controls the development of natural competence in *Streptococcus thermophilus* and *Streptococcus salivarius*. J Bacteriol **192:**1444-54.

23. **Chaffanel F, Charron-Bourgoin F, Libante V, Leblond-Bourget N, Payot S.** 2015. Resistance genes and genetic elements associated with antibiotic resistance in clinical and commensal isolates of *Streptococcus salivarius*. Appl Environ Microbiol **81:**4155-63.

24. **Bellanger X, Roberts AP, Morel C, Choulet F, Pavlovic G, Mullany P, Decaris B, Guédon G.** 2009. Conjugative transfer of the integrative conjugative elements ICE*St1* and ICE*St3* from *Streptococcus thermophilus*. J Bacteriol **191:**2764-75.

25. **Burrus V, Pavlovic G, Decaris B, Guédon G.** 2002. The ICE*St1* element of *Streptococcus thermophilus* belongs to a large family of integrative and conjugative elements that exchange modules and change their specificity of integration. Plasmid **48:**77-97.

26. **Carraro N, Libante V, Morel C, Decaris B, Charron-Bourgoin F, Leblond P, Guédon G.** 2011. Differential regulation of two closely related integrative and conjugative elements from *Streptococcus thermophilus*. BMC Microbiol **11:**238.

27. **van de Guchte M, van der Vossen JM, Kok J, Venema G.** 1989. Construction of a lactococcal expression vector: expression of hen egg white lysozyme in *Lactococcus lactis* subsp. *lactis*. Appl Environ Microbiol **55:**224-8.

28. **Aziz RK, Bartels D, Best AA, DeJongh M, Disz T, Edwards RA, Formsma K, Gerdes S, Glass EM, Kubal M, Meyer F, Olsen GJ, Olson R, Osterman AL, Overbeek RA, McNeil LK, Paarmann D, Paczian T, Parrello B, Pusch GD, Reich C, Stevens R, Vassieva O, Vonstein V, Wilke A, Zagnitko O.** 2008. The RAST Server: rapid annotations using subsystems technology. BMC Genomics **9:**75.

29. **Overbeek R, Olson R, Pusch GD, Olsen GJ, Davis JJ, Disz T, Edwards RA, Gerdes S, Parrello B, Shukla M, Vonstein V, Wattam AR, Xia F, Stevens R.** 2014. The SEED and the Rapid Annotation of microbial genomes using Subsystems Technology (RAST). Nucleic Acids Res **42:**D206-14.

30. **Carver T, Berriman M, Tivey A, Patel C, Bohme U, Barrell BG, Parkhill J, Rajandream MA.** 2008. Artemis and ACT: viewing, annotating and comparing sequences stored in a relational database. Bioinformatics **24:**2672-6.

31. **Sievers F, Wilm A, Dineen D, Gibson TJ, Karplus K, Li W, Lopez R, McWilliam H, Remmert M, Soding J, Thompson JD, Higgins DG.** 2011. Fast, scalable generation of high-quality protein multiple sequence alignments using Clustal Omega. Mol Syst Biol **7:**539.

32. **Tamura K, Stecher G, Peterson D, Filipski A, Kumar S.** 2013. MEGA6: Molecular Evolutionary Genetics Analysis version 6.0. Mol Biol Evol **30:**2725-9.

33. **Gouy M, Guindon S, Gascuel O.** 2010. SeaView version 4: A multiplatform graphical user interface for sequence alignment and phylogenetic tree building. Mol Biol Evol **27:**221-4.

34. **Blaiotta G, Sorrentino A, Ottombrino A, Aponte M.** 2011. Short communication: technological and genotypic comparison between *Streptococcus macedonicus* and *Streptococcus thermophilus* strains coming from the same dairy environment. J Dairy Sci **94:**5871-7.

35. **Lee CA, Grossman AD.** 2007. Identification of the origin of transfer (*oriT*) and DNA relaxase required for conjugation of the integrative and conjugative element ICE*Bs1* of *Bacillus subtilis*. J Bacteriol **189:**7254-61.

36. **Kishida K, Inoue K, Ohtsubo Y, Nagata Y, Tsuda M.** 2016. Host range of the conjugative transfer system of IncP-9 naphthalene-catabolic plasmid NAH7 and characterization of its *oriT* region and relaxase. Appl Environ Microbiol **83**. e02359-16. DOI: 10.1128/AEM.02359-16

663 37. **Wang P, Zhang C, Zhu Y, Deng Y, Guo S, Peng D, Ruan L, Sun M.** 2013. The resolution
664 and regeneration of a cointegrate plasmid reveals a model for plasmid evolution mediated by
665 conjugation and *oriT* site-specific recombination. Environ Microbiol **15:**3305-18.
666 38. **Ceccarelli D, Daccord A, Rene M, Burrus V.** 2008. Identification of the origin of transfer
667 (*oriT*) and a new gene required for mobilization of the SXT/R391 family of integrating
668 conjugative elements. J Bacteriol **190:**5328-38.
669 39. **Miyazaki R, van der Meer JR.** 2011. A dual functional origin of transfer in the ICE*clc*
670 genomic island of *Pseudomonas knackmussii* B13. Mol Microbiol **79:**743-58.
671 40. **Bose B, Auchtung JM, Lee CA, Grossman AD.** 2008. A conserved anti-repressor controls
672 horizontal gene transfer by proteolysis. Mol Microbiol **70:**570-82.
673 41. **Auchtung JM, Lee CA, Garrison KL, Grossman AD.** 2007. Identification and
674 characterization of the immunity repressor (ImmR) that controls the mobile genetic element
675 ICE*Bs1* of *Bacillus subtilis*. Mol Microbiol **64:**1515-28.
676 42. **Bellanger X, Morel C, Decaris B, Guédon G.** 2007. Derepression of excision of integrative
677 and potentially conjugative elements from *Streptococcus thermophilus* by DNA damage
678 response: implication of a cI-related repressor. J Bacteriol **189:**1478-1481.
679 43. **Carraro N, Libante V, Morel C, Charron-Bourgoin F, Leblond P, Guédon G.** 2016.
680 Plasmid-like replication of a minimal Streptococcal Integrative and Conjugative Element.
681 Microbiology **162:**622-632.
682 44. **Oliveira PH, Touchon M, Rocha EP.** 2014. The interplay of restriction-modification
683 systems with mobile genetic elements and their prokaryotic hosts. Nucleic Acids Res
684 **42:**10618-31.
685 45. **Mruk I, Kobayashi I.** 2014. To be or not to be: regulation of restriction-modification
686 systems and other toxin-antitoxin systems. Nucleic Acids Res **42:**70-86.

687 46. **Balado M, Lemos ML, Osorio CR.** 2013. Integrating conjugative elements of the
688 SXT/R391 family from fish-isolated Vibrios encode restriction-modification systems that
689 confer resistance to bacteriophages. FEMS Microbiol Ecol **83:**457-67.
690 47. **Price VJ, Huo W, Sharifi A, Palmer KL.** 2016. CRISPR-Cas and Restriction-Modification
691 act additively against conjugative antibiotic resistance plasmid transfer in *Enterococcus*
692 *faecalis*. mSphere **1(3):** e00064-16.
693 48. **Vasu K, Nagaraja V.** 2013. Diverse functions of restriction-modification systems in addition
694 to cellular defense. Microbiol Mol Biol Rev **77:**53-72.
695 49. **Rocha EP, Danchin A, Viari A.** 2001. Evolutionary role of restriction/modification systems
696 as revealed by comparative genome analysis. Genome Res **11:**946-58.
697 50. **Takahashi N, Naito Y, Handa N, Kobayashi I.** 2002. A DNA methyltransferase can protect
698 the genome from postdisturbance attack by a restriction-modification gene complex. J
699 Bacteriol **184:**6100-8.
700 51. **Jarup L, Akesson A.** 2009. Current status of cadmium as an environmental health problem.
701 Toxicol Appl Pharmacol **238:**201-8.
702 52. **Birri DJ, Brede DA, Nes IF.** 2011. Salivaricin D, a novel intrinsically trypsin-resistant
703 lantibiotic from *Streptococcus salivarius* 5M6c isolated from a healthy infant. Appl Environ
704 Microbiol **78:**402-10.
705 53. **Dobson A, Cotter PD, Ross RP, Hill C.** 2012. Bacteriocin production: a probiotic trait?
706 Appl Environ Microbiol **78:**1-6.
707 54. **Wescombe PA, Heng NC, Burton JP, Tagg JR.** 2009. Something old and something new:
708 an update on the amazing repertoire of bacteriocins produced by *Streptococcus salivarius*.
709 Probiotics Antimicrob Proteins **2:**37-45.

55. **Rankin DJ, Rocha EP, Brown SP.** 2011. What traits are carried on mobile genetic elements, and why? Heredity **106:**1-10.

56. **Bellanger X.** 2009. Transfert, accrétion et mobilisation des éléments intégratifs conjugatifs et des îlots génomiques apparentés de *Streptococcus thermophilus* : Un mécanisme clef de l'évolution bactérienne ? Ph. D. thesis. Nancy-Université, Nancy.

57. **Guédon E, Delorme C, Pons N, Cruaud C, Loux V, Couloux A, Gautier C, Sanchez N, Layec S, Galleron N, Almeida M, van de Guchte M, Kennedy SP, Ehrlich SD, Gibrat JF, Wincker P, Renault P.** 2011. Complete genome sequence of the commensal *Streptococcus salivarius* strain JIM8777. J Bacteriol **193:**5024-5.

58. **Jacob AE, Hobbs SJ.** 1974. Conjugal transfer of plasmid-borne multiple antibiotic resistance in *Streptococcus faecalis* var. zymogenes. J Bacteriol **117:**360-72.

59. **Takamatsu D, Osaki M, Sekizaki T.** 2001. Thermosensitive suicide vectors for gene replacement in *Streptococcus suis*. Plasmid **46:**140-8.

60. **Delorme C, Poyart C, Ehrlich SD, Renault P.** 2007. Extent of horizontal gene transfer in evolution of Streptococci of the salivarius group. J Bacteriol **189:**1330-41.

LEGENDS OF FIGURES

FIG 1 Comparison of the Integrative and Conjugative Elements (ICEs) found in *S. salivarius* and in other streptococci.

ICEs are named according to their host strain and integration site. ICEs of *S. salivarius* are indicated in bold. For more clarity, elements in accretion with ICEs are not shown. Nucleic sequence identity higher than 80% between sequences is indicated in light grey and higher than 90% in dark grey. Direct repeats (DR) delimiting ICEs are shown as a triangle, circle or square depending on their sequences. ORFs appear as arrows (truncated genes are indicated by Δ). Modules of recombination (integrase *int* and excisionase *xis* genes), conjugation (*orfA*-*orfO* genes) and regulation (including *arp1*, *arp2* and *orfQ* genes) appear in red, blue and green respectively. The three different integration genes (*fda*, *rpsI* or *rpmG*) targeted by the integrase are indicated by distinct symbols in the integrase gene and is stated in the ICE name. Genes from the adaptation module encoding proteins with putative function inferred from *in silico* analysis are indicated in color: in pink for RM systems and orphan methyltransferase genes, in dark grey for cadmium resistance genes (*cadD*/*X*), in yellow for the membrane lipid synthesis cluster, in orange for the bacteriocin synthesis cluster, in light green for genes encoding cell envelop proteins, in light pink for the cluster of genes for putative lipoprotein transport, in brown for the two component system (TCS), in black for the *tnp* transposase gene(s).

Sequences used for this analysis are: ICE*St3* of *S. thermophilus* [AJ586568] and sequenced genomes of *S. pneumoniae* 2842STDY5753514 [FDNK01000013], *S. macedonicus* 33MO [JNCV01000015] and *S. parasanguinis* DD19 [LQNY01000339-LQNY01000340]. Gaps in the assembly found in ICE*_SsaF6-1_rpsI*, ICE*_SsaB57_fda* and ICE*_SpaDD19_fda* are indicated by a double slash.

FIG 2 Phylogenetic BioNJ tree obtained for relaxases (OrfJ) of ICEs belonging to the ICE*St3* subfamily. The relaxase protein sequence of twenty-seven ICEs (the 19 ICEs of the ICE*St3* subfamily with closely related conjugation modules and 8 additional ones previously reported to belong to the same ICE subfamily but showing more distantly related conjugation modules) were included in the analysis. ICEs of *S. salivarius* are indicated in bold and *ICE_Sma33MO_fda* is indicated by a star. Bootstrap values supporting main branches are given for BioNJ/ML respectively.

FIG 3 Phylogenetic BioNJ tree obtained for coupling proteins (OrfK) of ICEs of the ICE*St3* subfamily. The sequence of the coupling protein of twenty-seven ICEs (the 19 ICEs of the ICE*St3* subfamily with closely related conjugation modules and 8 additional ones previously reported to belong to the same ICE subfamily but showing more distantly related conjugation modules) were included in the analysis. ICEs of *S. salivarius* are indicated in bold and *ICE_Sma33MO_fda* is indicated by a star. Bootstrap values supporting main branches are given for BioNJ/ML respectively.

FIG 4 PCR detection of integrated and excised forms of ICE*_SsaF1-4_fda*.
The sizes of the PCR fragments obtained for the amplification of the *attB, attI, attR* and *attL* sites (586 bp, 887 bp, 900 and 523 bp respectively) were confirmed by parallel migration of a DNA ladder. The primer pairs used for these amplifications are indicated in Table 2.

FIG 5 Characterization of transconjugants carrying ICE*_SsaF1-4_fda* after intraspecies transfer.
F1-4 (ICE*_SsaF1-4_fda*) was used as donor in mating experiments with (a) JIM8777 (pMG36e) and (b, c) F1-8 (pMG36e) as recipients. Tc. indicates transconjugants; integrase, amplification of the integrase gene of ICE*_SsaF1-4_fda*; pMG36e, amplification of an internal fragment of the pMG36e plasmid; RAPD, random amplification of polymorphic DNA; *attL, attR, attI and attB,* amplification

774 of fragments carrying these attachments sites in F1-8 transconjugants (c). The primer pairs used for
775 these amplifications are indicated in Table 2.
776
777 FIG 6 Characterization of transconjugants carrying ICE_*SsaF1-4_fda* after interspecies transfer.
778 F1-4 (ICE_*SsaF1-4_fda*) was used as donor in mating experiments with (a) LMG18311 (pMG36e)
779 and (b) JH2-2 (pMG36e) as recipients. Tc. indicates transconjugants; integrase, amplification of the
780 integrase gene of ICE_*SsaF1-4_fda*; ITS16S/23S, amplification of the internal transcribed spacer;
781 ITS16S/23S+*Hae*III digestion, amplification of the internal transcribed spacer followed by *Hae*III
782 digestion of the obtained fragment; EF *fda*, amplification of *fda* fragment using *E. faecalis* specific
783 primers.
784
785 FIG 7 Localization of the DNA cutting site of integrase by sequencing of *attR* site in *E. faecalis* JH2-
786 2 transconjugants.
787 ICE_*SsaF1-4_fda* is shown in green in its integrated form in donor *S. salivarius* strain F1-4 (upper
788 part of the figure), its excised form (middle part of the figure) and its integrated form in *E. faecalis*
789 JH2-2 recipient strain after transfer and integration (lower part of the figure). Nucleotide differences
790 in *att* sequences are indicated in green for ICE_*SsaF1-4_fda* and in red for *E. faecalis* JH2-2. The
791 position of the DNA cutting site of integrase deduced from this analysis is indicated by a black
792 arrow. A previous work aiming at studying CIME-ICE accretion also identified the same cutting
793 position as well as the position of a second staggered cutting site located 6 bp from the first one
794 (indicated in grey in the figure) (56).
795
796 FIG 8 Impact of mitomycin C on ICE_*SsaF1-4_fda* excision.

797 Fragments corresponding to the recombination sites *attB* and *attI* of non-treated (MMC-) or treated
798 (MMC+) cells were amplified by PCR using template DNA quantities ranging from 0.1 µg to 1 pg.
799 The amplification of the *fda* gene was used as a control.
800

TABLE 1 Bacterial strains and plasmids used in this study (to be continued)

Strains and plasmids	Relevant phenotype or genotype	Source or reference
Strains		
S. salivarius		
B35	Wild-type (WT) strain carrying a putative ICE of the ICE*St3* subfamily	(23)
B57	WT strain carrying a putative ICE of the ICE*St3* subfamily	(23)
F1-4	Wild-type (WT) strain carrying a putative ICE of the ICE*St3* subfamily (ICE_*SsaF1-4_fda*)	(23)
F1-4(ICE_*SsaF1-4_fda*) Cm^r	F1-4 carrying ICE_*SsaF1-4_fda* tagged with a Cm^r cassette	This work
F1-8	WT strain carrying a putative ICE in accretion with an IME integrated in the 3' end of *rpmG* , no element in *fda*	(23)
F1-8(pMG36e)	F1-8 carrying pMG36e, a plasmid conferring erythromycin resistance	This work
F4-2	WT strain carrying a putative ICE of the ICE*St3* subfamily	(23)
F6-1	WT strain carrying a putative ICE of the ICE*St3* subfamily	(23)
JIM8777	WT strain carrying a putative IME in the 3' end of *rpmG* and a putative CIME in the 3' end of *rpsI*, no element integrated in the *fda* gene	(57)
JIM8777(pMG36e)	JIM8777 carrying pMG36e, a plasmid conferring erythromycin resistance	This work
L22	WT strain carrying a putative ICE of the ICE*St3* subfamily	(23)
L50	WT strain carrying a putative ICE of the ICE*St3* subfamily	(23)
L60	WT strain carrying a putative ICE of the ICE*St3* subfamily	(23)
L64	WT strain carrying a putative ICE of the ICE*St3* subfamily	(23)
N5	WT strain carrying a putative ICE of the ICE*St3* subfamily	(23)
N20	WT strain carrying a putative ICE of the ICE*St3* subfamily	(23)
T93	WT strain carrying a putative ICE of the ICE*St3* subfamily	(23)
S. thermophilus		
CNRZ385 ICE*St3cat*	CNRZ385 carrying ICE*St3* with *cat* gene inserted in *orf385J* pseudogene, Cm^r	(24)
LMG18311	WT strain with no element in *fda*	BCCM/LMG
LMG18311(pMG36e)	LMG18311 carrying pMG36e, a plasmid conferring erythromycin resistance	(24)

TABLE 1 Bacterial strains and plasmids used in this study

Strains and plasmids	Relevant phenotype or genotype	Source or reference
E. faecalis		
JH2-2	WT strain with no element in *fda*	(58)
JH2-2(pMG36e)	JH2-2 carrying the plasmid pMG36e, conferring erythromycin resistance	(24)
Plasmids		
pSET5s	pWV01-type thermosensitive replication origin from pVE6002, LacZ, Cm^r	(59)
pMG36e	3.6 kb, replication origin from pWV01, Ery^r	(49)

TABLE 2. Primers used in this work (to be continued).

Primer use	Primer name	Sequence (5'-3')	Reference
ICE labeling			This study
	F1-4 CDS7 F	GAGATTGAGCATATCCTTCC	
	F1-4 CDS8 R_Bis	GGTGACTAGTTATCTACACGCGAGATTCGTGGACTAACTT	
	F1-4 CDS9 F_Bis	CCATATCCTTCTTTTTCTGCTCACTATCTTGTTCGTTTTGT	
	F1-4 CDS9 R	GGAGAGTTTAGCTGGGAGG	
	ICE F4-2 fragment I_F	GGAAATATCCTGTTGTCATC	
	ICE F4-2 fragtI_R-catbis	GGTGACTAGTTATCTACACGCCTATAAAGTTGTTAAGTTCACT	
	ICE F4-2 fragtII_F-catbis	CCATATCCTTCTTTTTCTGGCGTGTAATTGAAGAGTGA	
	ICE F4-2 fragment II_R	GTCTAAACTGAGCCAAGAAG	
	Cat_F	GCCTCCTAAATTCACTTTAG	
	Cat_R	GTAAAAAGTACAGTCGGCAT	
Detection of ICE integrated and excised forms			
attB amplification			(23)
	attBfdaSsal	GCCCAACCAAATAACACTAAA	
	attB ST3 Rev	CTCTTCGACCCACGTAAATTC	
attI amplification			(23)
	intST3 For	AGGGCTTTCTGACGAATTAG	
	attI ST3 Rev	CGGTGTAATGGGAAGTATGG	
attL amplification			
	attL Rv CDS gwlG	CGGTGTAATGGGAAGTATGG	This study
	attBfdaSsal	GCCCAACCAAATAACACTAAA	(23)
attR amplification			
	intST3 for	AGGGCTTTCTGACGAATTAG	(23)
	intICESt3-fdaRev	ACCAGGTTTCGATGCTATTACAG	(43)
Integrase gene			(23)
	intST3 for	AGGGCTTTCTGACGAATTAG	
	intST3 Rev	GAGTTCTAATAACTGAGGCTA	

TABLE 2. Primers used in this work

Primer use	Primer name	Sequence (5'-3')	Reference
Semi-quantitative PCR			
attI amplification			This study
	intICEF1-4 For	AGGTCTTTCTGACGAATTAG	
	attIICEF1-4 Rev	CGGCGTAATGGGAAGTATGG	
attB amplification			(23)
	attBfdaSsal	GCCCAACCAAATAACACTAAA	
	attB ST3 Rev	CTCTTCGACCCACGTAAATTC	
fda amplification			
	Fda1	TTCAAGAATTTACGTGGG	This study
	Fda2	AGATGCTAAAGCTATGGTTG	(34)
Donor / Recipient discrimination			
ITS16S/23S			(24)
	16SITS	TTGTACACACCGCCCGTCA	
	23SITS	GGTACCTTAGATGTTTCAGTTC	
ddlA gene			(60)
	ddlA up	TCAAGTGTGGCTATGGA	
	ddlA dn	GTAGATGGCTCCATCCTC	
E. faecalis fda specific amplification			(24)
	Efa fba1b	ATGTGTTCTTCTGCATCTTT	
	Efa fba2	CCCATTGATTACGATTTTT	
RAPD			(34)
	XD9	GAAGTCGTCC	
pMG36e			
	pMG36e Fwd	GCCTCCTCATCCTCTTCAT	(24)
	pMG36e_R	ACAGAACCGTTTCTACTCAATGAAC	This study

TABLE 3 Mating pairs tested in filter experiments

	Donor cells with AB^{r} [a]	Recipient cells with AB^{r} [a]
Intraspecies transfer	F1-4(ICE_*SsaF1-4_fda*) Cm^{r}	JIM8777 (pMG36e) Ery^{r} F1-8 (pMG36e) Ery^{r}
	F4-2(ICE_*SsaF4-2_fda*) Cm^{r}	JIM8777 (pMG36e) Ery^{r} F1-8 (pMG36e) Ery^{r}
Interspecies transfer	F1-4(ICE_*SsaF1-4_fda*) Cm^{r}	LMG18311 (pMG36e) Ery^{r} JH2-2 (pMG36e) Ery^{r}
	F4-2(ICE_*SsaF4-2_fda*) Cm^{r}	LMG18311 (pMG36e) Ery^{r} JH2-2 (pMG36e) Ery^{r}
ICE retransfer from transconjugants	F1-8(ICE_*SsaF1-4_fda*) Cm^{r}	F1-8 (pMG36e) Ery^{r} LMG18311 (pMG36e) Ery^{r}
	LMG18311(ICE_*SsaF1-4_fda*) Cm^{r}	LMG18311 (pMG36e) Ery^{r}
	JH2-2(ICE_*SsaF1-4_fda*) Cm^{r}	JH2-2 (pMG36e) Ery^{r}

[a] AB^{r} antimicrobial resistance of the strain

FIG 1

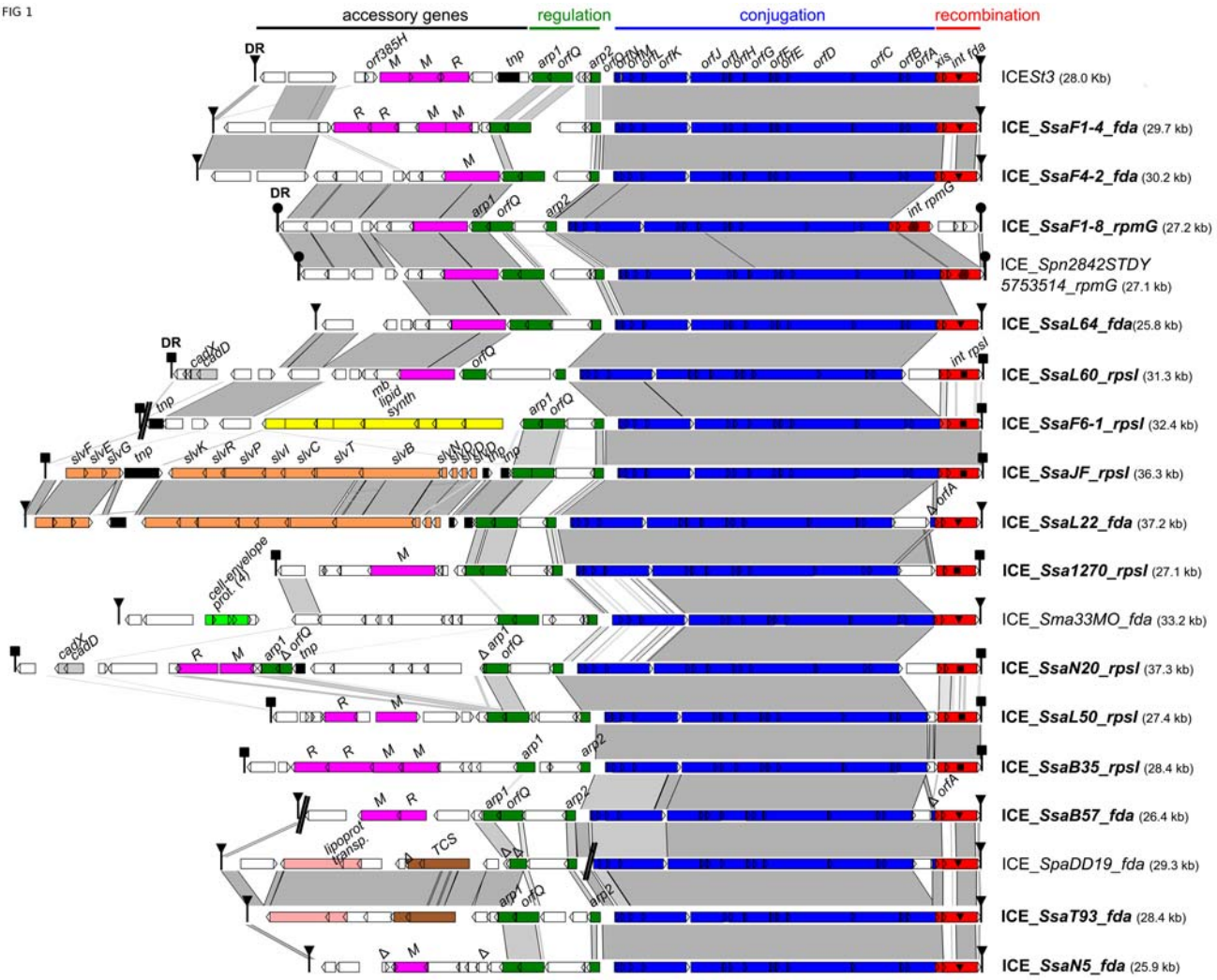
accessory genes
regulation
conjugation
recombination
DR
ICESt3 (28.0 Kb)
ICE_SsaF1-4_fda (29.7 kb)
ICE_SsaF4-2_fda (30.2 kb)
ICE_SsaF1-8_rpmG (27.2 kb)
ICE_Spn2842STDY 5753514_rpmG (27.1 kb)
ICE_SsaL64_fda(25.8 kb)
ICE_SsaL60_rpsI (31.3 kb)
ICE_SsaF6-1_rpsI (32.4 kb)
ICE_SsaJF_rpsI (36.3 kb)
ICE_SsaL22_fda (37.2 kb)
ICE_Ssa1270_rpsI (27.1 kb)
ICE_Sma33MO_fda (33.2 kb)
ICE_SsaN20_rpsI (37.3 kb)
ICE_SsaL50_rpsI (27.4 kb)
ICE_SsaB35_rpsI (28.4 kb)
ICE_SsaB57_fda (26.4 kb)
ICE_SpaDD19_fda (29.3 kb)
ICE_SsaT93_fda (28.4 kb)
ICE_SsaN5_fda (25.9 kb)

FIG 2

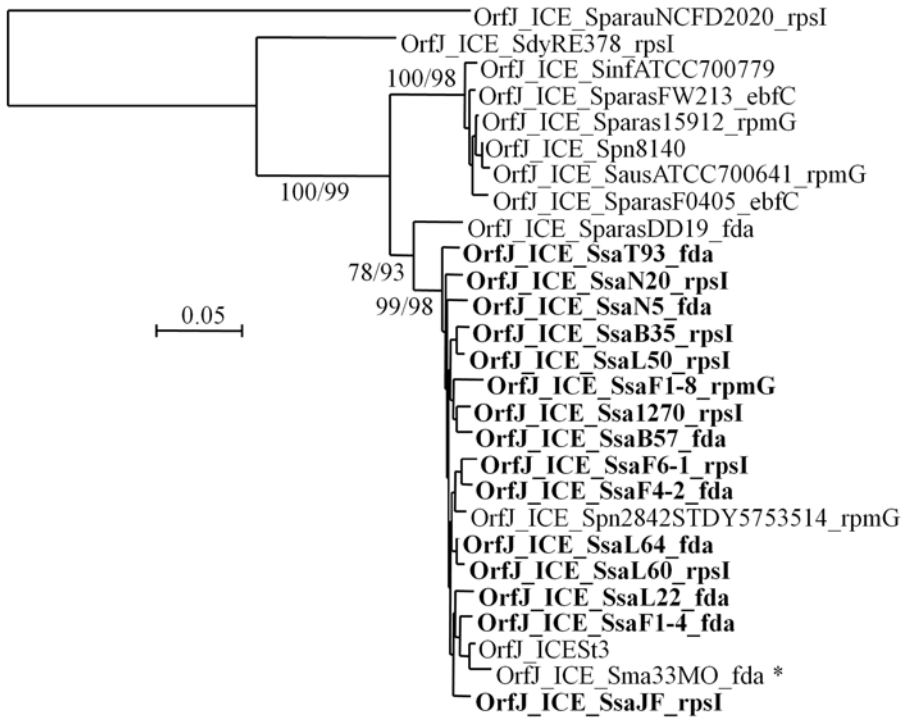
OrfJ_ICE_SparauNCFD2020_rpsI
OrfJ_ICE_SdyRE378_rpsI
100/98
OrfJ_ICE_SinfATCC700779
OrfJ_ICE_SparasFW213_ebfC
OrfJ_ICE_Sparas15912_rpmG
OrfJ_ICE_Spn8140
OrfJ_ICE_SausATCC700641_rpmG
100/99
OrfJ_ICE_SparasF0405_ebfC
OrfJ_ICE_SparasDD19_fda
78/93
OrfJ_ICE_SsaT93_fda
OrfJ_ICE_SsaN20_rpsI
99/98
OrfJ_ICE_SsaN5_fda
0.05
OrfJ_ICE_SsaB35_rpsI
OrfJ_ICE_SsaL50_rpsI
OrfJ_ICE_SsaF1-8_rpmG
OrfJ_ICE_Ssa1270_rpsI
OrfJ_ICE_SsaB57_fda
OrfJ_ICE_SsaF6-1_rpsI
OrfJ_ICE_SsaF4-2_fda
OrfJ_ICE_Spn2842STDY5753514_rpmG
OrfJ_ICE_SsaL64_fda
OrfJ_ICE_SsaL60_rpsI
OrfJ_ICE_SsaL22_fda
OrfJ_ICE_SsaF1-4_fda
OrfJ_ICESt3
OrfJ_ICE_Sma33MO_fda *
OrfJ_ICE_SsaJF_rpsI

FIG3

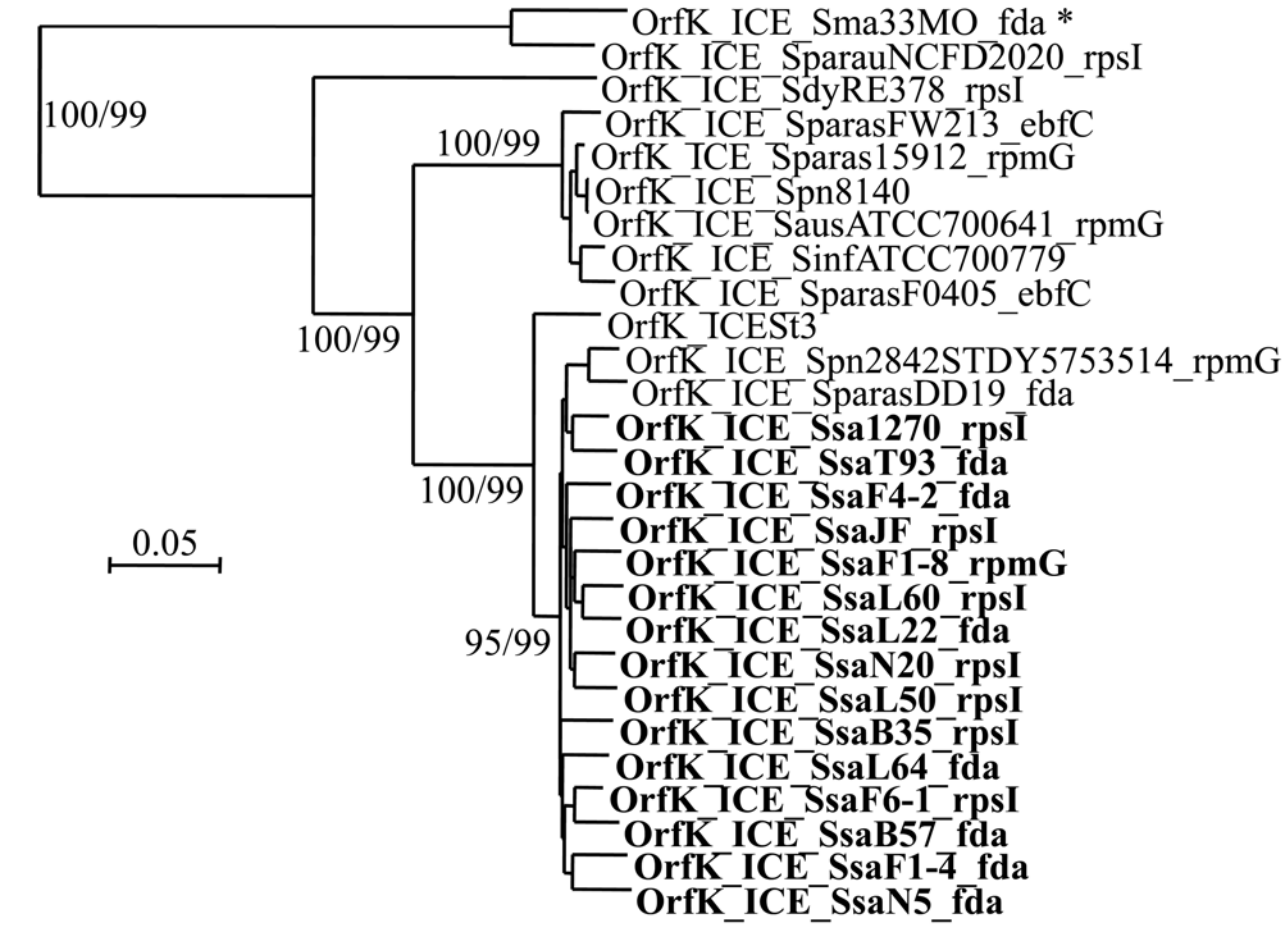
OrfK_ICE_Sma33MO_fda *
OrfK_ICE_SparauNCFD2020_rpsI
OrfK_ICE_SdyRE378_rpsI
OrfK_ICE_SparasFW213_ebfC
OrfK_ICE_Sparas15912_rpmG
OrfK_ICE_Spn8140
OrfK_ICE_SausATCC700641_rpmG
OrfK_ICE_SinfATCC700779
OrfK_ICE_SparasF0405_ebfC
OrfK_ICESt3
OrfK_ICE_Spn2842STDY5753514_rpmG
OrfK_ICE_SparasDD19_fda
OrfK_ICE_Ssa1270_rpsI
OrfK_ICE_SsaT93_fda
OrfK_ICE_SsaF4-2_fda
OrfK_ICE_SsaJF_rpsI
OrfK_ICE_SsaF1-8_rpmG
OrfK_ICE_SsaL60_rpsI
OrfK_ICE_SsaL22_fda
OrfK_ICE_SsaN20_rpsI
OrfK_ICE_SsaL50_rpsI
OrfK_ICE_SsaB35_rpsI
OrfK_ICE_SsaL64_fda
OrfK_ICE_SsaF6-1_rpsI
OrfK_ICE_SsaB57_fda
OrfK_ICE_SsaF1-4_fda
OrfK_ICE_SsaN5_fda
100/99
100/99
100/99
95/99
0.05

FIG 4

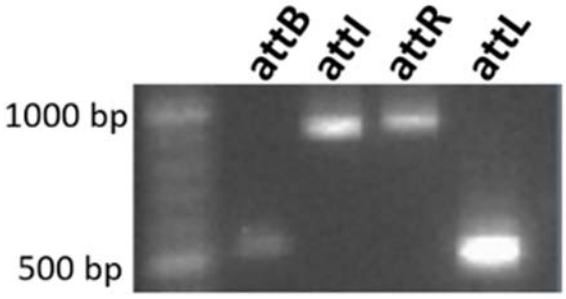

FIG5

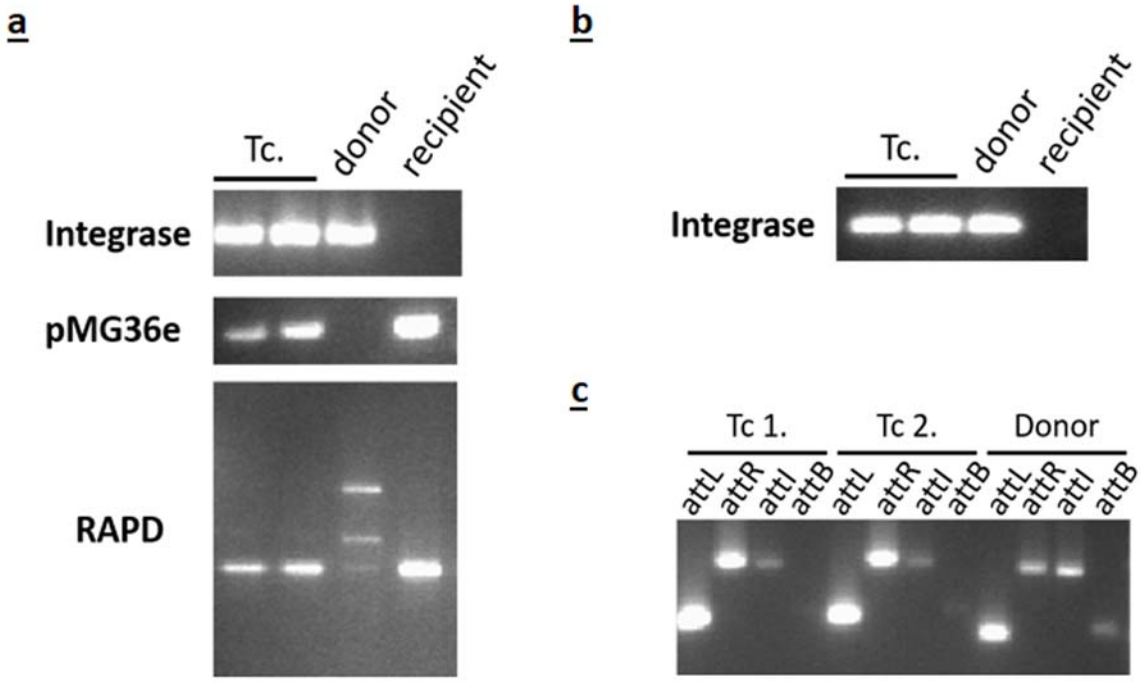
a
Tc.
donor
recipient
Integrase
pMG36e
RAPD
b
Tc.
donor
recipient
Integrase
c
Tc 1.
Tc 2.
Donor
attL
attR
attI
attB
attL
attR
attI
attB
attL
attR
attI
attB

FIG6

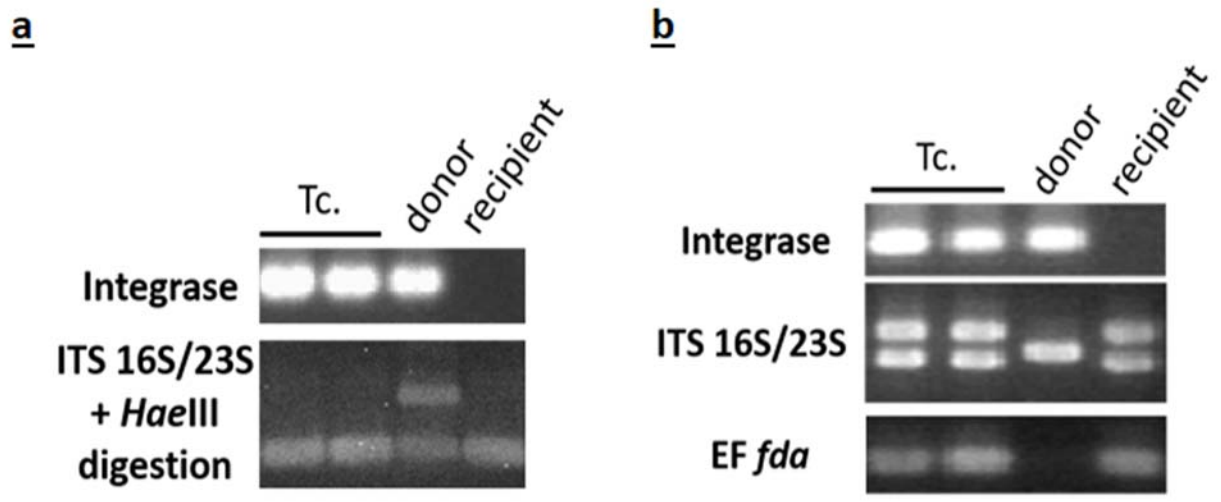
a
Tc.
donor
recipient
Integrase
ITS 16S/23S
+ HaeIII
digestion
b
Tc.
donor
recipient
Integrase
ITS 16S/23S
EF fda

FIG7

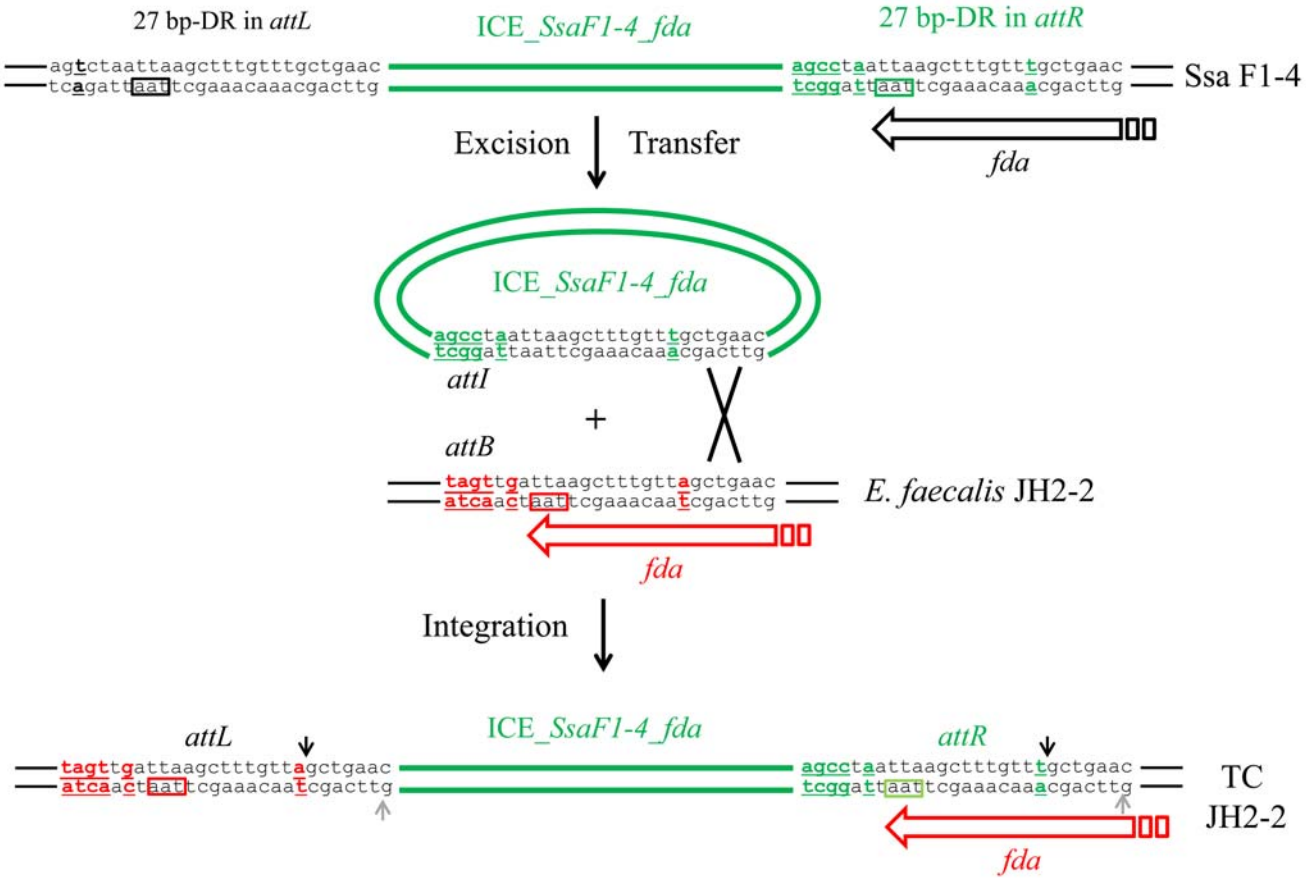
27 bp-DR in attL
ICE_SsaF1-4_fda
27 bp-DR in attR
agtctaattaagctttgtttgctgaac
tcagattaattcgaaacaaacgacttg
agcctaattaagctttgtttgctgaac
tcggattaattcgaaacaaacgacttg
Ssa F1-4
Excision
Transfer
fda
ICE_SsaF1-4_fda
agcctaattaagctttgtttgctgaac
tcggattaattcgaaacaaacgacttg
attI
+
attB
tagttgattaagctttgttagctgaac
atcaactaattcgaaacaatcgacttg
E. faecalis JH2-2
fda
Integration
attL
ICE_SsaF1-4_fda
attR
tagttgattaagctttgttagctgaac
atcaactaattcgaaacaatcgacttg
agcctaattaagctttgtttgctgaac
tcggattaattcgaaacaaacgacttg
TC
JH2-2
fda

FIG8

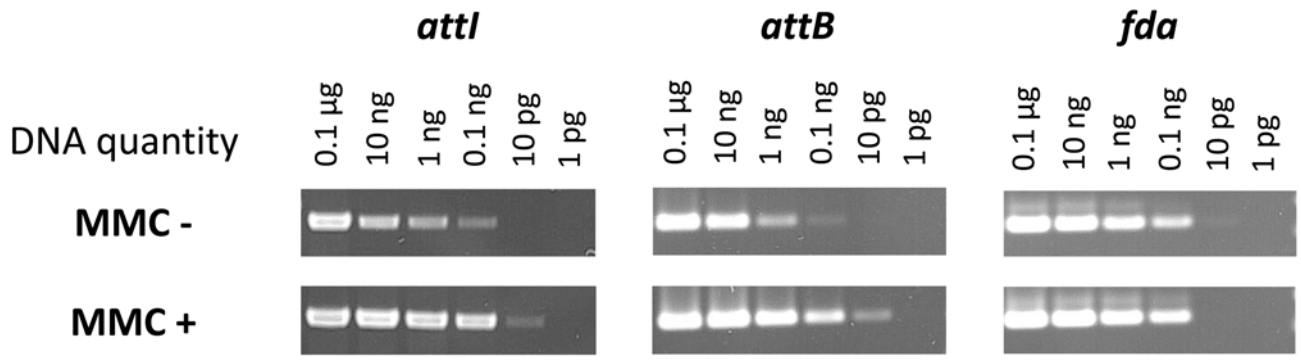
attI
attB
fda
DNA quantity
0.1 µg
10 ng
1 ng
0.1 ng
10 pg
1 pg
MMC -
MMC +

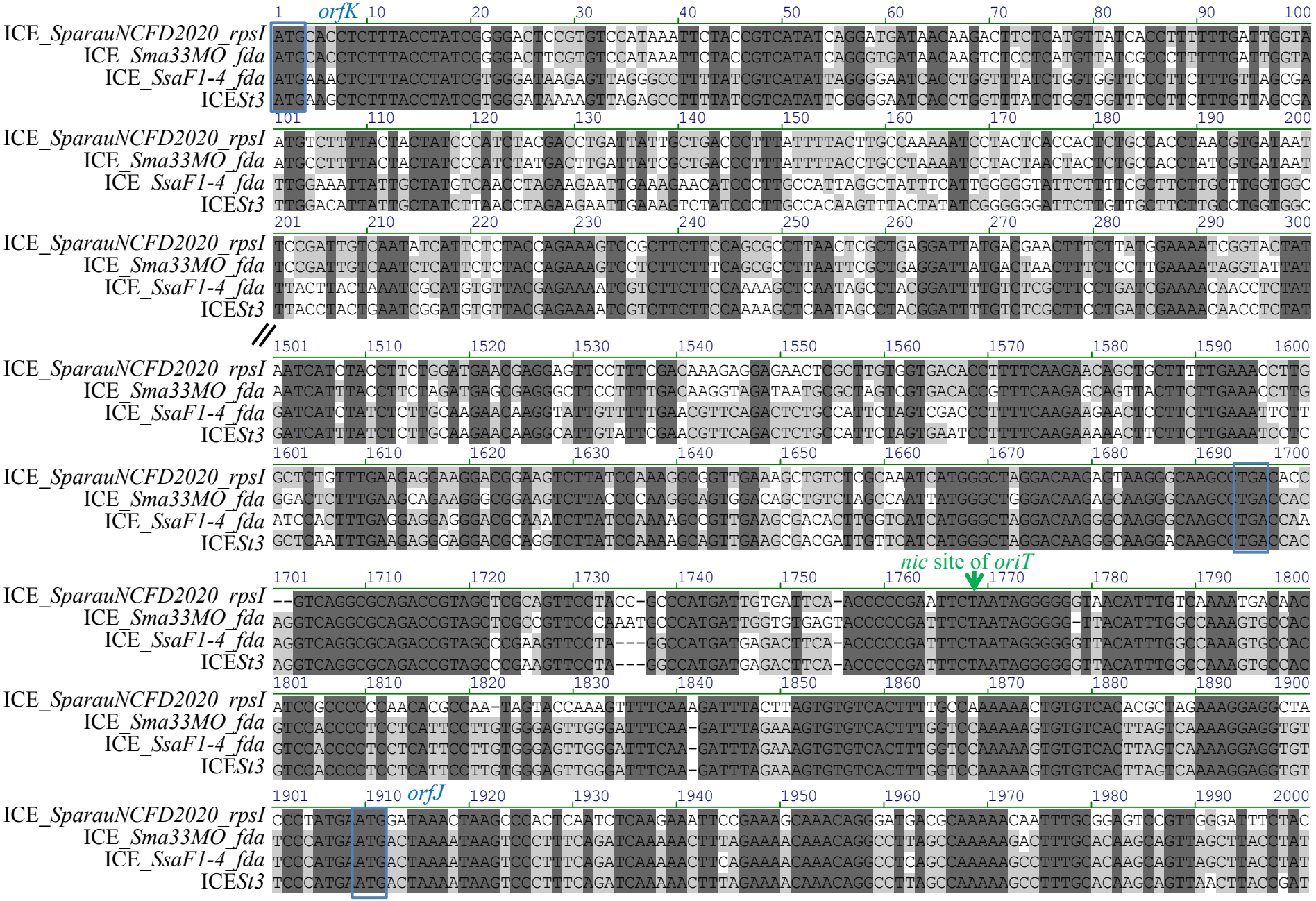

Fig. S1: sequence comparison of *orfK*, intergenic sequence *orfK-orfJ* and beginning of the *orfJ* gene in ICEs found in *S. parasanguinis* NCFD2020, *S. macedonicus* 33MO, *S. salivarius* F1-4 compared to ICE*St3* of *S. thermophilus*. Start and stop codons are indicated as blue rectangles and the *nic* site of *oriT* is indicated as a green arrow.

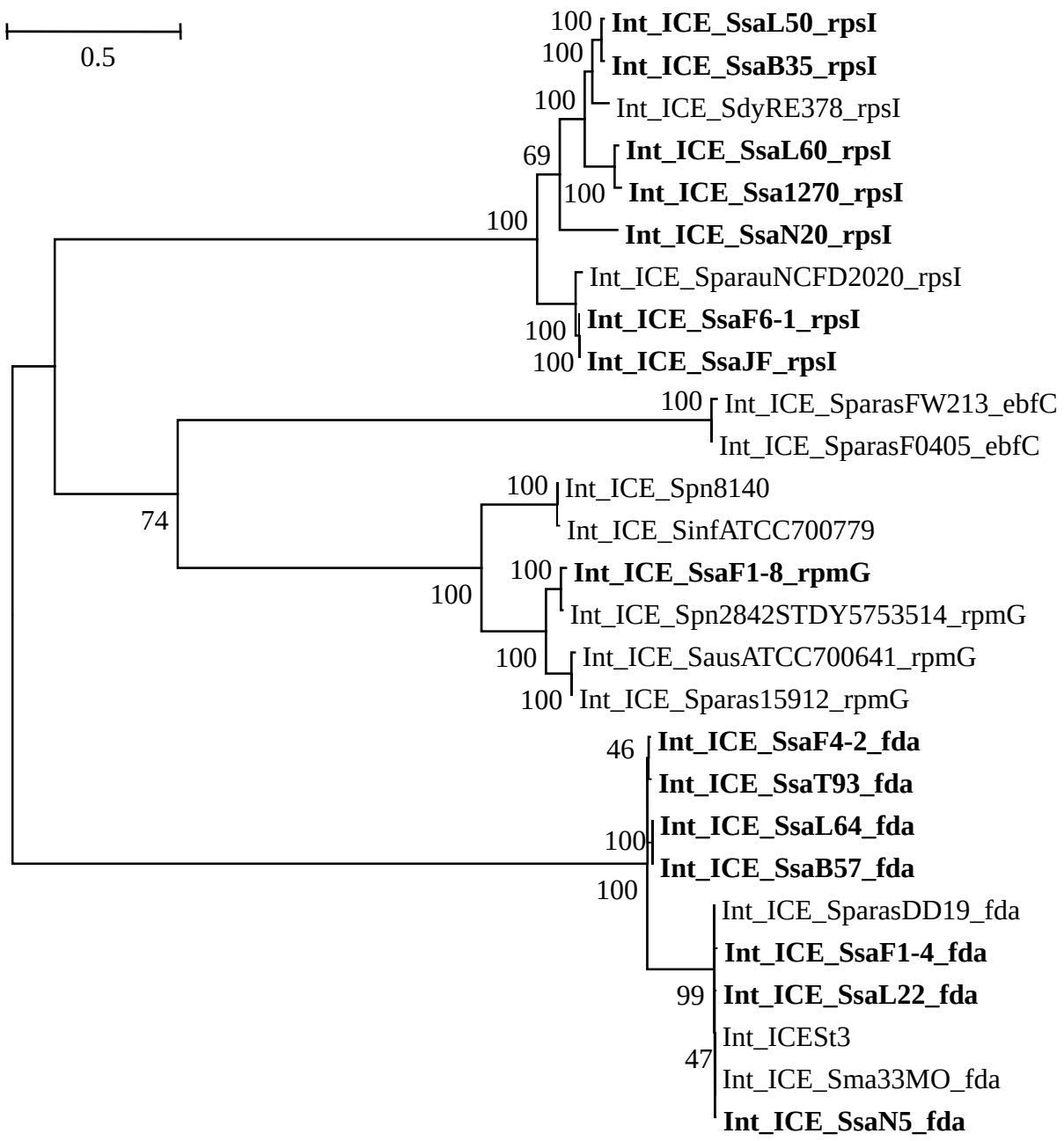

Fig. S2. Phylogenetic BioNJ tree obtained for integrases of ICEs belonging to the ICE*St3* subfamily. The integrase protein sequence of twenty-seven ICEs (the 19 ICEs of the ICE*St3* subfamily with closely related conjugation modules and 8 additional ones previously reported to belong to the same ICE subfamily but showing more distantly related conjugation modules) were included in the analysis. ICEs of *S. salivarius* are indicated in bold. Bootstrap values supporting main branches are given at nodes.